Physics – Uspekhi **37** (8) 715 – 737 (1994)

PACS numbers: 12.38. - t.

Quantum chromodynamics and multiplicity distributions

I M Dremin

Contents

Abstract. The quantum chromodynamics (QCD) approach to the problem of multiplicity distributions in high-energy particle collisions is described. The solutions of QCD equations for generating functions of the multiplicity distributions in gluon and quark jets are presented both for fixed and for running coupling constants. Characteristics have been found which are very sensitive to distribution shapes. The predictions are compared with experimental data. Evolution of the multiplicity distributions with decreasing phase space windows is considered and discussed in relation to the notions of intermittency and fractality. Some other QCD effects are briefly described.

1. Introduction

Quantum chromodynamics (QCD) has been treated for a long time as the theory of strong interactions. Its numerous successes in describing the static properties of hadrons (especially those of heavy quarkonia), the symmetry features of their interactions, and the sum rules are very impressive. The discovery of the asymptotic freedom of QCD has led to a theoretical foundation of the formerly phenomenological parton model and has opened the way for perturbation theory to be applied to hadron processes with high transferred momenta where quarks and gluons play the role of partons [1 – 5]. Certainly, the transition of quarks and gluons to experimentally accessible hadrons at the final stage of evolution should be considered, and we are still unable to treat it in a unique way since the problem of confinement has not been solved in the framework of QCD even though lattice calculations tell us that it is an inherent property of QCD. The simplified estimates show, however, that either this stage does not drastically change the final results, or its impact does not depend strongly on energy and therefore can be estimated from other processes at different energies. Phenomenologically, the distributions of partons and hadrons seem remarkably similar somehow. In such a situation, the study of the partonic stage of the cascade becomes of uppermost importance because the final properties of multiple production of hadrons at high energies are determined to a great extent by the partonic cascade.

The distribution of inelastic events according to the number of produced particles (the multiplicity distribution, for short) is one of the most important features revealing the dynamics of the interaction. Phenomenological approaches to its description usually originate from the simplified ideas about particle emission by several sources and exploit some distributions widely used in probability theory (see e.g. Ref. [6]). Among them, the negative binomial distribution is one of the most popular distribu-

I M Dremin P N Lebedev Physical Institute, 117924 Moscow
Tel. (095) 132-29-29

Received 4 March 1994
Uspekhi Fizicheskikh Nauk **164** (8) 785 – 809 (1994)
Submitted in English by the author; revised by J R Briggs

tions because it describes reasonably well the experimental data for various reactions in wide energy intervals, when its parameters are fitted, though there is some discrepancy at the highest accessible energies. The attractive feature of the negative binomial distribution is the Koba–Nielson–Olesen (KNO) scaling at asymptotically high energies, i.e. at average multiplicity tending to infinity. According to the KNO hypothesis [7], the multiplicity distributions depend on the ratio of the number of particles to the average multiplicity only (this is explained in more detail below). In its general features, this property has also been confirmed to a reasonable extent by experiment (with the possible exception of some data at the highest energies).

What does QCD tell us about multiplicity distributions? Some attempts to find an answer to this question have been made in the papers which constitute the main content of this review paper. It appears that QCD, when treated in higher-order approximations at the partonic level, has been able to predict some very delicate features of multiplicity distributions which happen to be qualitatively valid for hadrons as well. Before delving into the details of the conclusions, let us point out some 'underwater stones' and describe in brief the history of the problem.

First of all, one should always keep in mind that QCD provides conclusions about parton (quark and gluon) distributions but not about final hadrons, as has been mentioned already. One has to use additional assumptions to get from them the knowledge of experimentally accessible values. One of them is the hypothesis about the local parton–hadron duality [8], which claims that one should just renormalise the parton distributions without changing their shape to get hadron distributions. It originates from ideas of 'soft' preconfinement [9], when partons group in colourless clusters without disturbing the initial spectra. Phenomenological models of hadronisation have been attempted in Monte Carlo versions of inelastic processes and, in most cases, they support the approximate property of the local parton–hadron duality even though there exist some quantitative differencies from that hypothesis, as is described below.

Another problem, tightly connected to the first one, is the limitations of the perturbation theory analysis in a definite approximation. Formally speaking, one should apply perturbation theory only when the coupling constant is very small. That condition is fulfilled in QCD only for extremely large transferred momenta. In each process, however, the energy of cascading partons degrades during their evolution and one has to take proper account of soft partons, their recoil due to interaction, and energy–momentum conservation laws. All these factors used to be neglected in the lowest-order approximation when only the processes with a high gradient of energies and of emission angles at each stage of the evolution are considered (the so-called double-logarithmic approximation). Account is taken of soft partons and of strict angular ordering in the subsequent terms of the perturbation series, such as the modified leading-logarithm approximation and higher-order terms in the coupling constant. The recoil effects and conservation laws are also taken into account at that stage.

In most cases those corrections are well under control and are of the order of ten percent of the main term. In spite of their rather small total contribution, they are often very important and change the picture qualitatively in the region where the corresponding functions are small. For example, they are crucial for proper description of the multiple production processes. This manifests itself mathematically as a new expansion parameter equal to the product of the coupling constant (or, more precisely, of its square root) and the rank of the moment of the distribution. Thus, it is large at large ranks, i.e. at high multiplicity. These problems will be described in more detail in Sections 3–5.

That is why the very first results on the multiplicity distributions of partons in QCD were obtained by means of the double-logarithmic approximation (see reviews in Refs [5, 10]). They are both impressive and discouraging. First, they provide the asymptotic KNO scaling of the distributions, which does not depend on the value of the coupling constant at all [11]. One is tempted to speculate on a somewhat more general meaning of the result. However, it fails to be valid in higher-order approximations. The energy increase of the average multiplicity depends on the coupling constant. It is faster than any logarithmic function and slower than any power-like one (if the running coupling constant is used), which agrees quite well with experimental findings. At the same time, the shape of the KNO function contradicts all experimental distributions because it is much wider than any of them. Recently, it became possible to resolve the problem [12, 13] by proper consideration of the higher-order effects mentioned above. In any case, one can now state that the agreement with experiment is achieved at the qualitative level, at least. Moreover, some qualitative predictions of the perturbative QCD are unexpectedly well suited for 'soft' hadronic processes as well. On the other hand, it is puzzling even though one recognises that higher-order corrections should take into account ever softer partons in a consistent way. On the one hand, it probably implies the more general nature of soft and hard processes than has been imposed on various theoretical schemes and persuades us to reconsider our approaches to the origin of the effects under consideration (leading, for example, to the experimentally observed multiplicity distributions). In addition, the newly found characteristics prompted by solutions of the QCD equations are extremely sensitive to tiny details of the multiplicity distributions. The current state of affairs for the multiplicity distributions in quark and gluon jets described by QCD is the main concern of this article (see Sections 5–8).

Many discussions are devoted to the value of the ratio of average multiplicities in gluon and quark jets. The initial value obtained in the double-logarithmic approximation is 9/4. This strongly exceeds all experimental estimates. The simplest corrections reduce that value by about ten percent. An even larger decrease of this ratio has been predicted by the exact solution of the equations for the generating functions in the case of fixed coupling and by the higher-order approximations with a running coupling constant. Its derivation and correspondence to experimental data is discussed in Sections 6 and 7. The energy dependence of the average multiplicity is considered there also.

For the sake of completeness, one should mention other interesting facts concerning inelastic interactions of high-energy particles which are successfully described (and someTimes predicted) by QCD. Effects predicted by QCD are very exquisite, someTimes unexpected, and always extremely instructive. When studying the multiplicity distributions, one is eager to ask about their

behaviour not only in the total phase space but also in its smaller subregions. It is well known that these studies are very popular nowadays. They are related to the intermittency phenomenon and to the fractality of particle distributions within the small phase-space volume. This fractality results from wider fluctuations in such phase-space regions (for the latest review see [14]). Those features are caused by the relative widening of the multiplicity distributions in smaller phase-space volumes. It gives rise to the increase of their moments in a power-like manner directly revealing properties of intermittency and fractality. Such tendencies have been experimentally observed. QCD describes the increase of the moments, relates the intermittency exponents (or fractal dimensions) directly to the anomalous dimension and clearly depicts the region of applicability of those regularities indicating the scales at which one should take into account the running coupling constant or consider it as a fixed one. These results are described briefly in Section 8.

The quantum-mechanical origin of the interacting partons reveals itself in various interference effects. They lead to the hump-backed plateau of rapidity distributions, to the correlations of partons in energies and azimuthal angles, to the string (or drag) effect in the three-jet events and in the production of heavy bosons and lepton pairs at large transverse momenta, and to the suppression of the forward production of accompanying particles in processes with heavy quarks. These are described briefly in Section 9. Unfortunately, the details of interactions with nuclei as well as interactions of polarised quarks are not mentioned in this paper to keep it to a reasonable size. They deserve a separate article.

My main concerns here are the multiplicity distributions and related characteristics. I apologise to the authors of numerous papers on multiplicity distributions whose contribution has not been mentioned. My only excuse stems from the intention to describe just the QCD approach to the subject. In addition, omissions can happen unintentionally, unfortunately.

2. Definitions and notation

The distribution of the number of particles produced in high-energy inelastic events is called the multiplicity distribution and is given by the formula

$$P_n = \frac{\sigma_n}{\sum_{n=0}^{\infty} \sigma_n}, \tag{1}$$

where σ_n is the cross section of n-particle production processes (the so-called topological cross section) and the sum is over all possible values of n so that

$$\sum_{n=0}^{\infty} P_n = 1. \tag{2}$$

SomeTimes it is more convenient to replace the multiplicity distribution by its moments, i.e. by another set of numbers obtained from it by a definite algorithm. All such sets can be obtained from the so-called generating function defined by the formula

$$G(z) = \sum_{n=0}^{\infty} P_n (1+z)^n, \tag{3}$$

which substitutes an analytic function in place of the set of numbers P_n.

In what follows, use will often be made of the (normalised) factorial moments F_q and cumulants K_q determined from the generating function $G(z)$ by the relations

$$F_q = \frac{\sum_n P_n n(n-1)\ldots(n-q+1)}{\left(\sum_n P_n n\right)^q} = \frac{1}{\langle n\rangle^q} \frac{\mathrm{d}^q G(z)}{\mathrm{d}z^q}\bigg|_{z=0}, \tag{4}$$

$$K_q = \frac{1}{\langle n\rangle^q} \frac{\mathrm{d}^q \ln G(z)}{\mathrm{d}z^q}\bigg|_{z=0}, \tag{5}$$

where

$$\langle n\rangle = \sum_{n=0}^{\infty} P_n n \tag{6}$$

is the average multiplicity. The expression for $G(z)$ can be rewritten as

$$G(z) = \sum_{q=0}^{\infty} \frac{z^q}{q!} \langle n\rangle^q F_q \quad (F_0 = F_1 = 1), \tag{7}$$

$$\ln G(z) = \sum_{q=1}^{\infty} \frac{z^q}{q!} \langle n\rangle^q K_q \quad (K_1 = 1). \tag{8}$$

The distribution P_n and its ordinary moments C_q are derived from the generating function $G(z)$ according to the formulas

$$P_n = \frac{1}{n!} \frac{\mathrm{d}^n G(z)}{\mathrm{d}z^n}\bigg|_{z=-1}, \tag{9}$$

$$C_q = \frac{\sum_{n=0}^{\infty} P_n n^q}{\langle n\rangle^q} = \frac{1}{\langle n\rangle^q} \frac{\mathrm{d}^q G(\exp z - 1)}{\mathrm{d}z^q}\bigg|_{z=0}. \tag{10}$$

All the moments are connected by definite relations that can easily be derived from their definitions in terms of the generating function. For example, the factorial moments and cumulants are related to each other by the identities

$$F_q = \sum_{m=0}^{q-1} C_{q-1}^m K_{q-m} F_m, \tag{11}$$

which are nothing other than the relations between the derivatives of a function and of its logarithm at the point where the function itself equals 1. Here

$$C_{q-1}^m = \frac{(q-1)!}{m!(q-m-1)!} = \frac{\Gamma(q)}{\Gamma(m+1)\Gamma(q-m)} = \frac{1}{mB(q,m)} \tag{12}$$

are the binomial coefficients, and Γ and B denote the gamma- and beta-functions, respectively. Thus there are only numerical coefficients in the recurrence relations (11) and the iterative solution (well-suited for computer calculation) reproduces all cumulants if the factorial moments have been given, and vice versa. In that sense, cumulants and factorial moments are equally suitable. The physical meaning of both of them is clearly seen from their

definitions if they are presented in the form of integrals of correlation functions. However I will not include them here (for a review, see Ref. [14]) but shall instead refer to the analogous relations in quantum field theory where formulas similar to Eqns (4) and (5) define the complete set of Feynman graphs (both connected and disconnected) and the subset of connected diagrams, respectively (see e.g. Ref. [1]). Thus, it is easy to recognise that the factorial moments are the integral characteristics of any correlations among the particles while the cumulants of qth rank correspond to 'genuine' q-particle correlations not reducible to the product of lower-order correlations†. To be more precise, all q particles are connected to each other in the qth cumulant and cannot be split into disconnected groups. One can say that they form a q-particle cluster which is not divided into smaller clusters, in analogy with Mayer cluster decomposition in statistical mechanics.

It is a common feature of distributions in particle physics that their factorial moments and cumulants increase rapidly at large ranks q. That is why it is convenient to consider their ratio

$$H_q = \frac{K_q}{F_q}, \tag{13}$$

which behaves in a more 'quiet' way at high ranks q, at the same time emphasising all the typical qualitative peculiarities of cumulants as functions of their rank q.

Using the definition of factorial moments, Eqn (4), one can easily derive their relation to the ordinary moments C_q of the same and lower ranks. The coefficients depend on the mean multiplicity so that, for example,

$$F_2 = \frac{\langle n(n-1)\rangle}{\langle n\rangle^2} = C_2 - \langle n\rangle^{-1}. \tag{14}$$

This complicates the whole matter since one has to recalculate them at any given energy if the F scaling persists. That is why the ordinary moments are not used in what follows. In the asymptotics, the ordinary and factorial moments coincide, however.

One should keep in mind that the generating function contains the same physical information as the multiplicity distribution. This is true also for unnormalised moments and for their ratio. For normalised moments, one should define the average multiplicity at a given energy. Note that the higher-rank moments lay emphasis on higher-multiplicity events. The multiplicities $n \geqslant q$ contribute to the factorial moment of the (integer) rank q, as is seen from Eqn (4). If the distribution is cut off at some $n = n_{\max}$, all factorial moments with the rank $q > n_{\max}$ are equal to zero, while they are positive at smaller q. The cumulants may be either positive or negative.

Up to now, without mentioning it, it has been assumed that the rank of the moment is a positive integer. However, the definitions (4), (5), and (10) can be generalised to include noninteger moments [15]. This is easily done by rewriting the factorial moments as

$$F_q = \frac{1}{\langle n\rangle^q}\sum_{n=0}^{\infty} P_n \frac{\Gamma(n+1)}{\Gamma(n-q+1)}, \tag{15}$$

†This interpretation is valid, however, only for moments with rank smaller than the average multiplicity at a given energy (for more details, see the review paper Ref. [14]).

which is valid at any real value of the rank q. One can obtain the same formula by forming the derivative of real order q (i.e. by using fractional calculus) of the generating function.

According to the generalised differentiation rule one gets a fractional derivative of any (real) order if the complete set of ordinary derivatives of integer order is known [16]:

$$\mathrm{D}_z^q G(z) = \sum_{m=0}^{\infty} \frac{(1+z)^{m-q} G^{(m)}(-1)}{\Gamma(m-q+1)}, \tag{16}$$

where $G^{(m)}(-1)$ is the derivative of the (positive) integer order m of the function $G(z)$, defined by Eqn (3), at $z = -1$. The generalised definition of factorial moments for any real (positive and negative) noninteger and integer q can be written as:

$$F_q = \frac{1}{\langle n\rangle^q}\mathrm{D}_z^q G(z)\Big|_{z=0} = \frac{1}{\langle n\rangle^q}\sum_{m=0}^{\infty}\frac{G^{(m)}(-1)}{\Gamma(m-q+1)}. \tag{17}$$

Eqns (9), (15), and (17) correspond to each other, i.e. the experimental definition of factorial moments given by Eqn (15) is equivalent to its theoretical definition given by Eqn (17) as the fractional derivatives of the generating function. At integer ranks one gets the previously used formulas. That is why the generalised (to noninteger ranks) moments are known as fractional moments. Their use could help distinguish various distributions, as discussed later.

The situation with cumulants is more complicated. It is straightforward to define [17] them theoretically as

$$K_q = \frac{1}{\langle n\rangle^q}\mathrm{D}_z^q \ln G(z)\Big|_{z=0} = \frac{1}{\langle n\rangle^q}\sum_{m=0}^{\infty}\frac{(\ln G(z))^{(m)}|_{z=-1}}{\Gamma(m-q+1)}. \tag{18}$$

However, the relation between factorial moments and cumulants becomes much more complicated than formula (11) and impractical to use. We should keep in mind that the aim here is not to calculate the cumulants themselves but to find the characteristics of multiplicity distributions which are most sensitive to their shape. Therefore, it has been proposed to use the so-called 'analytically continued' cumulants denoted by $K_q^{(a)}$ and defined by the following recursion relations at any real rank q:

$$F_q = \sum_{m=0}^{[q-1]} \frac{k_{q-m}^{(a)} F_M}{mB(q,m)}. \tag{19}$$

The sum is up to the integer part of $q-1$. As is easily seen from formulas (11) and (12), it can be used for any value of q, integers included. It is convenient both for experimentalists and for theorists, after some additional convention. The relation to the 'true' cumulants defined by Eqn (18) has been lost, however.

3. Phenomenology

3.1 KNO scaling and F scaling

One of the most successful assumptions about the shape of the multiplicity distributions at high energies is the hypothesis that the energy dependence is determined completely by the behaviour of the average multiplicity in such a way that the distribution P_n may be represented as:

$$P_n = \frac{1}{\langle n\rangle} f\left(\frac{n}{\langle n\rangle}\right). \tag{20}$$

This property has been called KNO scaling after the names of its authors [7] who proposed it on the basis of the Feynman plateau of rapidity distributions. The normalisation condition (2) leads to

$$\int_0^\infty f(x)\,\mathrm{d}x = 1 . \tag{21}$$

It is clear that the ordinary moments of the KNO distribution (20) do not depend on energy and are just functions of their rank q:

$$C_q = \int_0^\infty x^q f(x)\,\mathrm{d}x = \mathrm{const}(E) . \tag{22}$$

The factorial moments of the distribution are energy dependent and tend to constant values at asymptotically high energies because they differ from the ordinary moments by lower-order correlation terms suppressed by the inverse of the average multiplicity to the corresponding power. Constancy of the factorial moments will be called F scaling. It coincides with KNO scaling in asymptotics. As is clear from definitions (3), (7), and (8), the generating function depends only on the average multiplicity in both cases.

In QCD with a fixed coupling constant (see Section 7), F scaling is preferred. However, the difference from KNO scaling is usually neglected since the theoretical calculations are often performed for asymptotically high energies. The preasymptotic correction terms in the second moment have been considered in Ref. [18].

In the double-logarithmic approximation the equations for factorial moments are independent of both energy and coupling constant. The corresponding function $f(x)$ decreases exponentially [5] at large values of x:

$$f(x) \sim 2\mathrm{C}\left(\mathrm{C}x - 1 + \frac{1}{3\mathrm{C}x} + \ldots\right)\exp(-\mathrm{C}x) , \quad \mathrm{C}x \gg 1 , \tag{23}$$

where $C \approx 2.553$. At low low values of x it behaves as

$$f(x) \sim x^{-1}\exp\left(-\frac{1}{2}\ln^2 x\right) . \tag{24}$$

Though the very appearance of KNO scaling and its independence of the coupling constant in the lowest approximation are by themselves a great success of perturbative QCD [11], the shape of the scaling function (23) does not fit experimentally obtained shapes. Experiment favours the shapes which are much narrower than is prescribed by Eqns (23) and (24). The corrections of the modified leading-logarithmic approximation indicate that the resulting form should become less wide [19]. It happens that the higher-order terms reduce the width of $f(x)$ but it now depends on the coupling constant. Those problems are treated in Sections 5–7.

Up to now, it has been implicitly assumed that the multiplicity distributions are being treated in the total phase space. It is reasonable to consider the question of their evolution if some restrictions are imposed on the region of the phase space under investigation. In particular, one can study such distributions in ever smaller rapidity intervals contained within the total interval. In that case, the moments of the distribution become, in general, functions of the size of the interval as well as of their ranks (for a review, see Ref. [14]). Their behaviour is often related to the notions of intermittency and fractality discussed briefly in Section 9.

3.2 Conventional distributions

We shall consider three distributions in which analytic expressions for generating functions and all moments can be derived [20, 21]. They will serve as the 'starting points' for further discussion of QCD distributions. First, we shall describe the moments of integer rank, and then show what happens with arbitrary (fractional, negative, complex rank) moments.

3.2.1 Poisson distribution. The presence of correlations in a process is conventionally described by the difference between its typical distribution and the Poisson distribution, which is written as

$$P_n = \frac{\langle n\rangle^n}{n!}\exp(-\langle n\rangle) . \tag{25}$$

The generating function is [see Eqn (3)]

$$G(z) = \exp(\langle n\rangle z) , \tag{26}$$

and, according to Eqns (4) and (5), one gets

$$F_q = 1 , \quad K_q = H_q = \delta_{q1} . \tag{27}$$

Therefore the measure of correlations could be defined as the difference between F_q and 1, or between K_q (H_q) and 0. There is exact F scaling and asymptotic KNO scaling.

The fractional (in general, complex rank) factorial moments of the Poisson distribution [15] are

$$F_q = \frac{\exp(-\langle n\rangle)}{\langle n\rangle^q \Gamma(1-q)}\Phi(1,\,1-q\,;\,\langle n\rangle) , \tag{28}$$

where Φ is the degenerate confluent hypergeometric function. At positive integer values of q they are equal to 1, as they should be, and oscillate with an amplitude depending on q and $\langle n\rangle$ in the intervals between the integer ranks, as it is shown in Fig. 1 (curve *5*).

The cumulants [17] are

$$K_q = \frac{q}{\langle n\rangle^{q-1}\Gamma(2-q)} , \tag{29}$$

and the ratios are

$$H_q = \frac{q}{1-q}\frac{\langle n\rangle\exp(\langle n\rangle)}{\Phi(1,1-q;\langle n\rangle)} . \tag{30}$$

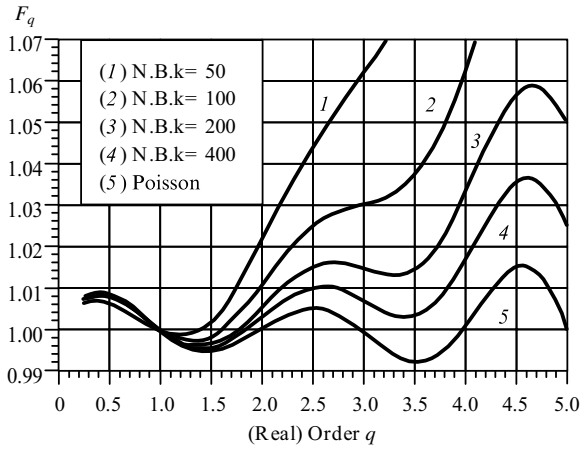

Figure 1. Fractional factorial moments [15] of Poisson (*5*) and negative binomial distributions (*1–4*, correspond to various values of k) with the average multiplicity $\langle n\rangle = 2$. The amplitude of oscillations decreases strongly at larger $\langle n\rangle$ and smaller k.

One gets Eqn (27) from Eqns (28), (29), and (30) at positive integer q. The amplitude of oscillation of the moments decreases rapidly with increasing average multiplicity. In fact, they originate from quite simple properties of the gamma-function in the denominator.

At large average multiplicity all factorial moments tend to 1 in the whole complex plane q. However, the cumulants tend to zero only at $\mathrm{Re}\, q > 1$ and increase in absolute value at $\mathrm{Re}\, q < 1$ with the increase of mean multiplicity, which can be used for analysis of distributions in the total phase space at high energies. Qualitative features of that kind are typical for other distributions considered below.

3.2.2 The negative binomial distribution. The negative binomial distribution (NBD) deserves special attention because it has been actively used for the last several years to fit the experimental multiplicity distributions and has been rather successful. In particular, there is a widely spread opinion that it describes almost all inelastic processes at high energies (except for data at the highest available energies, i.e. for e^+e^- at 91 GeV — DELPHI [22], OPAL [23] — and for proton–antiproton interactions at energies from 200 to 900 GeV — UA5 [24]). For NBD we have

$$P_n = \frac{\Gamma(n+k)}{\Gamma(n+1)\Gamma(k)} \left(\frac{\langle n\rangle}{k}\right)^n \left(1+\frac{\langle n\rangle}{k}\right)^{-n-k}, \tag{31}$$

where k is an adjustable parameter with the physical meaning of the number of independent sources. The Bose–Einstein distribution is a special case of NBD with $k = 1$. The Poisson distribution is obtained from Eqn (31) in the limit $k \to \infty$. The generating function is

$$G(z) = \left(1 - \frac{z\langle n\rangle}{k}\right)^{-k}, \tag{32}$$

and the (integer rank) moments are

$$F_q = \frac{\Gamma(k+q)}{\Gamma(k)k^q}, \tag{33}$$

$$K_q = \frac{\Gamma(q)}{k^{q-1}}, \tag{34}$$

$$H_q = \frac{\Gamma(q)\Gamma(k+1)}{\Gamma(k+q)} = kB(q,k). \tag{35}$$

At a fixed value of k, the rate of increase with q of the factorial moments is greater than that of the exponents. The cumulants are steeply decreasing at small q until they reach a minimum at $q \approx k$ and start increasing at larger q. They always stay positive. Note that the product of several generating functions of negative binomial distributions with different parameters also leads to positive cumulants since the unnormalised total cumulant is just the sum of unnormalised individual cumulants. The ratio H_q is also positive and decreases monotonically (as q^{-k} at large q).

Fig. 2 shows the behaviour of $\ln F_q$, $\ln K_q$, and $\ln H_q$ as functions of q for $k = 5$ and 10. Since P_n is narrower at higher k, the slower rise of F_q for $k = 10$ compared with that for $k = 5$ is expected. The dependence of K_q on k is more pronounced than that of H_q. These properties are more characteristic of NBD than general and do not reveal themselves in QCD.

It should be noted that the NBD with fixed parameter k possesses F scaling (the moments do not depend on energy) and the asymptotic KNO scaling. The KNO function at large n and fixed values of k behaves as

$$f(x) = \frac{k^k}{(k-1)!} x^{k-1} \exp(-kx). \tag{36}$$

The generating function (91) is singular at the point $z = k/\langle n\rangle \to 0$ for $\langle n\rangle \to 0$ and $k = \mathrm{const}$. Therefore, we have to work in the vicinity of the singularity when calculating its derivatives at $z = 0$ (factorial moments). The singularity moves closer to $z = 0$ at higher energies.

The general expressions for the moments valid for any rank q in the entire complex plane are

$$F_q = \frac{(kv)^k}{\langle n\rangle^{q+k}} \frac{F(1,\, k;\, 1-q;\, v)}{\Gamma(1-q)} = \frac{F(k,\, -q;\, 1-q;\, -\langle n\rangle/k)}{\langle n\rangle^q \Gamma(1-q)}, \tag{37}$$

$$K_q = \frac{k}{\langle n\rangle^q \Gamma(1-q)} \left[\frac{v}{1-q} F(1,\, 1;\, 2-q;\, v) + \ln\frac{kv}{\langle n\rangle}\right], \tag{38}$$

$$H_q = k\left(\frac{\langle n\rangle}{kv}\right)^k \frac{v(1-q)^{-1}F(1,\, 1;\, 2-q;\, v) + \ln(kv/\langle n\rangle)}{F(1,\, k;\, 1-q;\, v)}, \tag{39}$$

where $v = \langle n\rangle/(\langle n\rangle + k)$.

The oscillations of moments between integer values of q diminish at higher average multiplicities (i.e. at higher energies) and at lower values of k. This is shown in Fig. 1 (curves *1–4*) for F_q. They are really very small at high energies. The oscillations are imposed on the rapid increase of F_q with q.

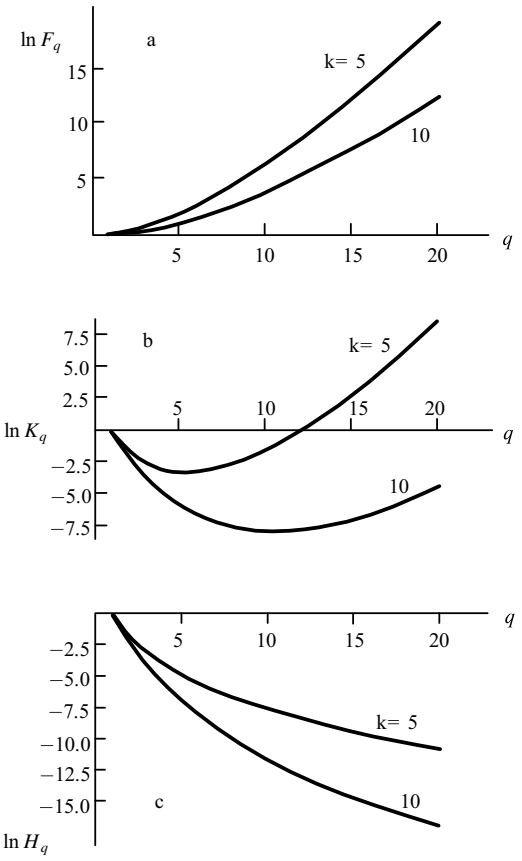

Figure 2. Moments of the negative binomial distribution [21] for $k = 5$ and 10 calculated for integer values of q. The curves are drawn to guide the eye. (a) $\ln F_q$, (b) $\ln K_q$, (c) $\ln H_q$.

At negative values of q the moments increase with average multiplicity. In the complex plane, their oscillations are noticeable (for example, along lines parallel to the real axis).

3.2.3 Fixed multiplicity distribution. The case of fixed multiplicity is considered just to show that the behaviour of moments (even for integer ranks) can drastically differ from the examples treated above. In addition, it demonstrates how important the role of the selection procedure in experiments could be. In fact events with a given multiplicity are often chosen for analysis (so called semi-inclusive events), i.e. one deals with the distribution

$$P_n = \delta_{nn_0} \qquad (n_0 = \text{const}) \; . \tag{40}$$

Then one gets

$$G(z) = (1+z)^{n_0} \; . \tag{41}$$

Since $\langle n \rangle = n_0$, one obtains

$$F_q = \frac{n_0!}{n_0^q (n_0 - q)!} = \frac{\Gamma(n_0) n_0^{1-q}}{\Gamma(n_0 - q + 1)} \; , \quad 1 < q \leqslant n_0 \; , \tag{42}$$

$$F_q = 0 \; , \quad q > n_0 \; , \tag{43}$$

$$K_q = (-n_0)^{1-q} (q-1)! = (-n_0)^{1-q} \Gamma(q) \; , \tag{44}$$

$$H_q = (-1)^{1-q} n_0 B(q, n_0 - q + 1) \; . \tag{45}$$

All factorial moments of rank higher than n_0 are identically zero and one can calculate H_q at $q \leqslant n_0$ only. The typical feature of that distribution is the alternating signs of integer-order cumulants, which are positive at odd values of q and negative at even values. The amplitude of oscillations decreases when q increases from 1 to n_0 and then increases monotonically. A change of sign (but with a different periodicity) will be seen in QCD as well. Factorial moments, however, behave differently in the two cases. They decrease monotonically with q until n_0 for fixed multiplicity and increase rapidly in QCD.

Fig. 3 shows F_q, K_q, H_q for $n_0 = 10$, and (in the insets) $\ln|K_q|$ and $\ln|H_q|$ for integer values of q. Straight lines connect just the points at integer values of q and are shown to guide the eye.

It should be stressed that the very existence of the oscillations can be related just to the selection procedure of the events and, in the case of fixed multiplicity, has nothing to do with the dynamics of the interaction. It is easy to recognise when one chooses e.g. 10-particle events from the set of those with Poisson distribution (or any other). Then we obtain alternating-sign cumulants at integer ranks instead identically equal to zero. Their amplitude can preserve the information on the original distribution if its normalisation has been kept untouched.

The fractional moments calculated according to their definitions at any rank q are

$$F_q = n_0^{1-q} \frac{B(n_0, 1-q)}{\Gamma(1-q)} \; , \tag{46}$$

$$K_q = n_0^{1-q} \frac{\psi(1) - \psi(1-q)}{\Gamma(1-q)} \; , \tag{47}$$

$$H_q = \frac{\psi(1) - \psi(1-q)}{B(n_0, 1-q)} \; . \tag{48}$$

For fixed q and $n_0 \to \infty$ one gets $F_q \to 1, K_q \to 0, H_q \to 0$.

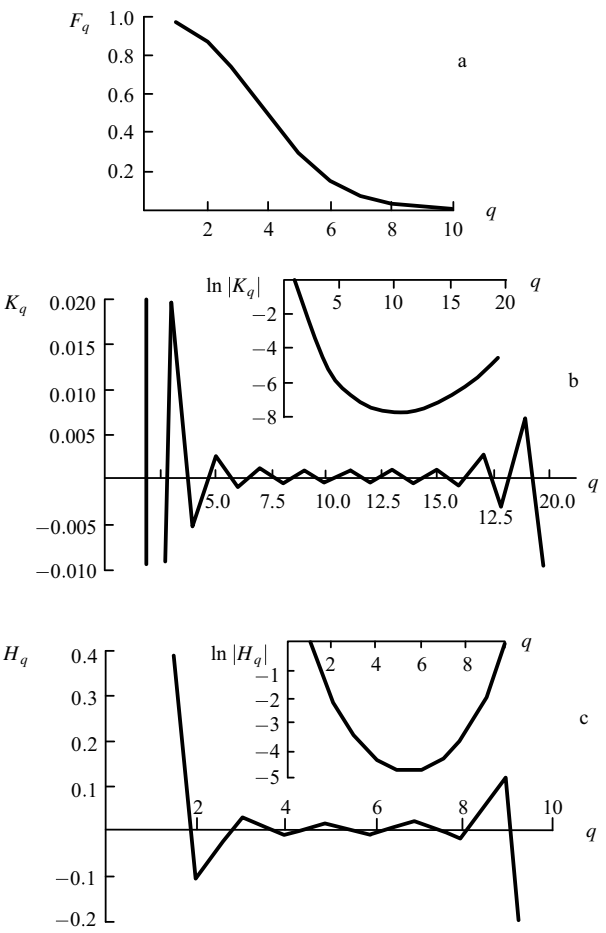

Figure 3. Moments of fixed multiplicity distribution [21] for $n_0 = 10$ calculated for integer values of q. The curves are drawn to guide the eye. (a) F_q, (b) K_q, $\ln|K_q|$, (c) H_q, $\ln|H_q|$.

Let us stress that in all the cases considered the noninteger-rank moments are not obtained by the simple-minded 'analytic continuation' according the formula (19) but are given by the various expressions [compare Eqn (27) with Eqns (28)–(30), Eqns (33)–(35) with Eqns (37)–(39), or Eqns (42)–(45) with Eqns (46)–(48)] which are derived from the proper definitions (17) and (18).

The common property of oscillations between the integer ranks is the change from maximum to minimum at each subsequent rank. At the integer points, there are knots for Poisson and negative binomial distributions and just maxima or minima for fixed multiplicity.

Unfortunately, the oscillations between the integer ranks are small at high multiplicity and can be useful for distributions with low average multiplicity like those in the small phase-space volumes considered in Section 9. At high multiplicity they impose low-amplitude harmonics on the main dependence, and may be neglected in the first approximation.

Also, the increase of the negative moments with average multiplicity can be useful for analysis of distributions within the total phase space.

3.3 Some models

At first sight, the graph-theoretic description of multiparticle production looks completely different in e^+e^- and hadron–hadron processes. In the former case, main graphs

are of the tree-like type with a highly virtual initial parton. In the latter case, one used to consider a sequence of multiperipheral-type graphs with low virtualities and rather complicated topology. A more general (and unifying) picture emerges from consideration of strings between the colour charges in the process of their interaction (Lund model [22, 23], dual topological model [24, 25], quark–gluon string model [26, 27]) and of final particles clusterisation (multiperipheral cluster model [28], clans [6, 29] etc.). The multiplicity distributions in the models are not usually described by a single analytic formula but are formed from a combination of several distributions. For example, the multiperipheral model with a single ladder gives rise to the Poisson distribution of the particle emission centres (resonances, fireballs, clusters, clans, etc.). In general, the resulting distribution is obtained by convolution of the Poisson distribution of the number of sources with the decay distribution which describes experimental data quite well enough for educated guesses about decay properties to be made. If one chooses the logarithmic distribution of cluster decay multiplicity then its convolution with the Poisson distribution of clusters produces a negative binomial distribution of final particles multiplicities. The simultaneous creation of several ladders (or strings) gives rise to a more complicated shape of the distribution. SomeTimes this distribution may be approximated by a sum of negative binomial distributions with distinct parameters. As a result, distributions with 'shoulders' or 'quasi-oscillations' imposed on smooth curves can be observed. The possible relation between such oscillations and those of H_q discussed here has been considered in Ref. [30]. Similarly, a single jet in e^+e^- annihilation can give rise to a negative binomial distribution while the superposition of several jets differs from it in the resulting distribution [31]. The detailed study of those semiphenomenological models is usually performed with Monte Carlo computations.

4. Equations of quantum chromodynamics

Multiparticle production processes are described in QCD as a result of the interaction of quarks and gluons, which leads to the creation of additional quarks and gluons forming the observed hadrons at the final stage. The most typical features of the processes are determined by the vector nature of gluons and by the dimensionless coupling constant. Gluons are colour charged in distinction to photons, which have no electric charge. Therefore, they can emit gluons in addition to quark–antiquark pairs. That is why both quark and gluon jets are considered in QCD as main objectives. Their development is described by the evolution equations. The main parameter of the evolution is the angle of divergence of the jet or its transverse momentum. The subsequent emission of gluons and quarks fills in the internal regions of the previously developed cones so that they do not overlap (angular ordering). This remarkable property can be exploited to formulate a probabilistic scheme for the development of the jet as a whole. Then its evolution equations are reminiscent of the well-known classical Markovian equations for the 'birth–death' (or 'mother–daughter') processes. (For a detailed discussion of that approach, based on the coherence phenomenon, see Ref. [5]).

The system of two equations for the generating functions G_F and G_G of the quark and gluon jets, respectively, are (with A, B, C = F, G) [1, 5]

$$G_A(y,z) = \exp[-w_A(y)]z + \frac{1}{2}\sum_{B,C}\int^y \mathrm{d}y' \int_0^1 \mathrm{d}x \exp[-w_A(y)+w_A(y')] \times \frac{\alpha_S}{2\pi} K_A^{BC}(x) G_B(x, y') G_C[(1-x), y'] , \quad (49)$$

where $y = \ln(p\Theta/Q_0)$, p is an initial momentum, Θ is the angle of divergence of the jet, $Q_0 = \mathrm{const}$, and α_S is the coupling constant. The first term on the right-hand side corresponds to the propagation of the primary parton without any evolution and is described by the form factor $\exp[-w_A(y)]$. The second term shows the creation of two jets B and C with proportions of the primary energy x and $1-x$, respectively, after their production at the vertex K_A^{BC} with the evolution parameter y', which has been reached by the primary parton without splitting as is dictated by the factor $\exp[-w_A(y)+w_A(y')]$.

Multiplying both sides of the equation by $\exp[w_A(y)]$ and differentiating over y, we get rid of all form factors and obtain the final system of equations [1, 5]:

$$G_G' = \int_0^1 \mathrm{d}x\, K_G^G(x)\gamma_0^2\{G_G(y+\ln x)G_G[y+\ln(1-x)] - G_G(y)\} + n_f\int_0^1 \mathrm{d}x\, K_G^F(x)\gamma_0^2\{G_F(y+\ln x)G_F[y+\ln(1-x)] - G_G(y)]\}, \quad (50)$$

$$G_F' = \int_0^1 \mathrm{d}x K_F^G(x)\gamma_0^2\{G_G(y+\ln x)G_F[y+\ln(1-x)] - G_F(y)\}, \quad (51)$$

where $G'(y) = \mathrm{d}G/\mathrm{d}y$, and n_f is the number of active flavours,

$$\gamma_0^2 = \frac{6\alpha_S}{\pi}, \quad (52)$$

and the kernels of the equations are

$$K_G^G(x) = \frac{1}{x} - (1-x)[2-x(1-x)], \quad (53)$$

$$K_G^F(x) = \frac{1}{4N_c}[x^2 + (1-x)^2], \quad (54)$$

$$K_F^G(x) = \frac{C_F}{N_c}\left(\frac{1}{x} - 1 + \frac{x}{2}\right), \quad (55)$$

where $N_c = 3$ is the number of colours, and $C_F = \frac{1}{2}N_c(1-N_c^{-2}) = \frac{4}{3}$ in QCD.

The variable z has been omitted in the generating functions. One should keep in mind, however, that the deriva-tion of the equations for the moments relies completely on the expansions (7) and (8) when they are inserted into the above equations and the coefficients in front of terms z^q are compared.

A typical feature of any field theory with a dimensionless coupling constant (QCD in particular) is the presence of the singular terms at $x \to 0$ in the kernels of the equations. They imply the uneven sharing of energy between newly created jets and play an important role in jet evolution.

Even though the system of equations (50) and (51) is physically appealing, it is not absolutely exact; i.e. it is not derived from first principles of QCD. One immediately notices this since, for example, there is no four-gluon interaction term contained in the Lagrangian of QCD. Such a term would not lead to a singular contribution to the kernels and its omission is justified in the lowest orders. Nevertheless, the modified series of the perturbation theory (with three-parton vertices) is well reproduced by such equations up to the terms involving two-loop and three-loop corrections. As shown in Ref. [5], the neglected terms would contribute at the level of the product of, at least, five generating functions. Physical interpretation of the corresponding graphs would lead to treatment of the 'colour polarisability' of jets. There are some problems with the definition of the evolution parameter, with preasymptotic corrections etc. (see, e.g., [32]). The above arguments do not prevent from further detailed studies of higher order corrections to these equations, and it seems reasonable to learn more about the solutions of the equations with higher accuracy since there are indications that neglected terms are not very important.

5. Gluodynamics

It is natural to start our studies with the simplest case of gluodynamics, in which there are no quarks and interactions of only gluons are considered. The system of equations (50) and (51) degenerates to the single equation

$$G'(y) = \int_0^1 \mathrm{d}x\, K(x)\gamma_0^2 \{G(y + \ln x)G[y + \ln(1-x)] - G(y)\}\ , \tag{56}$$

where $G(y) \equiv G_{\mathrm{G}}(y)$, $K(x) \equiv K_{\mathrm{G}}^{\mathrm{G}}(x)$. This is a nonlinear integrodifferential equation with shifted arguments in the nonlinear term which take into account the energy conservation. In the lowest-order double-logarithmic approximation, one considers the most singular terms in the kernel $K(x)$ and within the curly brackets, i.e. $1/x$ in K and $\ln(1-x) \to 0$, while γ_0^2 is chosen to be constant†.

5.1 Approximate solutions of equations with fixed coupling constant and the shape of the KNO function

Formally, the assumptions of the double-logarithmic approximation for each of the three terms under the integral sign in Eqn (56) are equivalent because one neglects nonleading contributions. A detailed analysis of these terms has been performed in many papers [9–13, 21, 32–37], individually or in combination. In most papers only the lower moments have been treated, i.e. the average multiplicity and the dispersion. It has been noticed that the role of the conservation laws displayed in the shifted arguments of the generating functions is the most important one. They provide larger corrections. It was shown recently [12] that they could be precisely taken into account. However, the running property of the coupling constant was disregarded, the nonsingular terms in the kernel were neglected (as well as some other terms) and the difference between the coupling constant γ_0 (52) and the QCD anomalous dimension γ, defined as

†Somewhat inconsistently, the running coupling constant is someTimes considered in that approximation also (see e.g. [1, 5]).

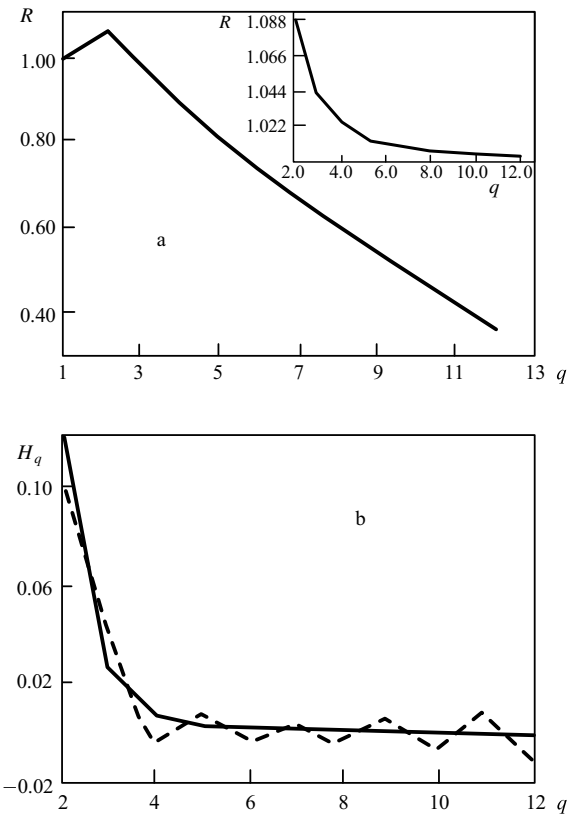

Figure 4. (a) The ratio of the factorial moments as derived from Eqn (5) to the asymptotic values of Eqn (7) (inset) and the similar ratio as derived from the KNO curve (see Fig. 5) and Eqn (7) (the main part). (b) The ratio H_q obtained from the KNO curve (Fig. 5) (solid line) as compared with its NBD counterpart for $k = 7$ (dashed line). (I am indebted to B B Levtchenko, who provided this figure especially for this review.)

$$\langle n \rangle = \exp \int^y \gamma(y')\,\mathrm{d}y'\ , \tag{57}$$

was neglected also. In Section 7, it is shown that Eqns (50) and (51) possess the exact solutions for fixed coupling constant without any additional assumptions. Nevertheless, it is instructive to consider this case because one gets the analytic expression for the KNO function which clearly reveals the importance of the conservation laws and differs from formula (23) for the double-logarithmic approximation by a narrower width, thus getting much closer to experimental values.

First, one obtains a recurrence relation for the factorial moments when relations (7) are substituted in Eqn (56) and the coefficients of z^q are equated on both sides:

$$(q - q^{-1})F_q = \gamma \sum_{l=1}^{q-1} C_q^l B[\gamma l,\ \gamma(q-l)+1]F_{q-l}F_l\ . \tag{58}$$

This system can be computed‡ with the initial conditions $F_0 = F_1 = 1$. The inset of Fig. 4a shows the ratio of these moments to the asymptotic solution [12] of Eqns (58):

$$F_q^{as} = \frac{[\Gamma(1+\gamma)]^q}{\Gamma(1+\gamma q)} \frac{2q\Gamma(q+1)}{C^q}\ . \tag{59}$$

‡The exact solution of the system of equations for quark and gluon jets is given in Section 7.2.

At large values of $q\gamma$ one obtains

$$F_q \approx \frac{2\mu D^{-q}}{\sqrt{2\pi\gamma}}\Gamma\left(\frac{3}{2}+\frac{q}{\mu}\right), \tag{60}$$

where

$$\mu = (1-\gamma)^{-1}, \quad D = \frac{C\gamma^{\gamma}(1-\gamma)^{1-\gamma}}{\Gamma(1+\gamma)}.$$

The asymptotics of F_q determines the asymptotics of the KNO function $f(x)$:

$$f(x) \approx \frac{2\mu^2(Dx)^{3\mu/2}}{x\sqrt{2\pi\gamma}}\exp[-(Dx)^{\mu}], \quad (\mu-1)(Dx)^{\mu} \gg 1. \tag{61}$$

Clearly, the tail of the distribution at large multiplicities is suppressed far more strongly than in the double-logarithmic approximation. One gets an 'almost Gaussian' suppression instead of the exponent in Eqn (23) if one considers the practically important values of γ for which $\mu = (1-\gamma)^{-1} \approx 1.6$. Thus, we conclude that conservation laws drastically reduce the width of the multiplicity distribution. This is demonstrated in Fig. 5, where the modified distribution (which takes into account the behaviour at low multiplicities [12]) is compared with the results of the lowest order QCD and with its fit by the negative binomial distribution with the parameter $k = 7$. Making use of the modified curve in Fig. 5, one is able to compute the 'genuine' (with low-multiplicity correction) factorial moments. Their ratio to the asymptotic solution (59) is shown in the main part of Fig. 4a. Comparison of the two curves in that figure reveals the important influence of corrections made at low multiplicities. From 'genuine' factorial moments, one can compute cumulants and the 'genuine' ratio H_q (the latter is shown in Fig. 4b and compared with the negative binomial distribution prediction for $k = 7$ and $\langle n\rangle = 30$). One notices a visible departure from the negative binomial distribution in the ratios H_q, while it is hard to see this in the distributions shown in Fig. 5. The oscillations of 'genuine' H_q are in contrast to its smooth behaviour in the negative binomial distribution. Here they are somewhat reminiscent of the fixed multiplicity toy-model considered above. Similar shapes with oscillations of different (!) periodicity will be discussed in what follows.

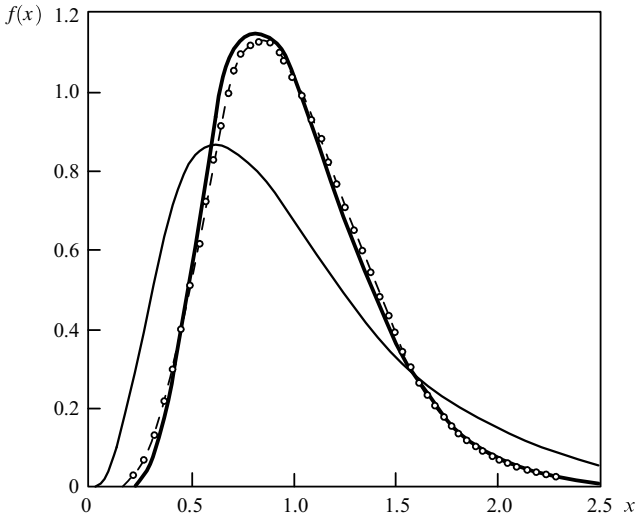

Figure 5. The modified KNO function [12] (thick curve) for $\gamma = 0.4$ is much narrower than the lowest order distribution (thin line). The negative binomial distribution with $k = 7$ is also shown for comparison (dots).

5.2 Higher-order approximations with running coupling constant

The equation (56) for the generating function in gluodynamics can be solved in a somewhat different approximation by taking into account all (including nonsingular) terms of the kernel K, by considering all running coupling constant γ_0 distinct from the anomalous dimension γ, and by using the Taylor series expansion for the generating functions in the nonlinear term at large y:

$$G(y+\varepsilon) \approx G(y) + G'(y)\varepsilon + \tfrac{1}{2}G''(y)\varepsilon^2 + \ldots. \tag{62}$$

This approach clearly shows the distinction between the various assumptions, and their importance and qualitative effects due to the higher-order corrections.

Using expression (62) for the generating functions in the nonlinear term of Eqn (56), dividing both sides of it by $G(y)$ and differentiating with respect to y, we obtain

$$[\ln G(y)]'' = \gamma_0^2\left[G(y) - 1 - 2h_1G'(y) + \sum_{n=2}^{\infty}(-1)^n h_n G^{(n)}(y) + \sum_{m,n=1}^{\infty}(-1)^{m+n}h_{nm}\left(\frac{G^{(m)}G^{(n)}}{G}\right)'\right], \tag{63}$$

where

$$h_1 = \frac{11}{24}, \quad h_n = |2 - 2^{-n} - 3^{-n} - \zeta(n)|,$$

$$\zeta(n) = \sum_{m=1}^{\infty} m^{-n}, \quad n \geqslant 2, \tag{64}$$

$$h_{mn} = \left|\frac{1}{m!\,n!}\int_0^1 \mathrm{d}x\, K(x)\ln^n(x)\ln^m(1-x)\right|. \tag{65}$$

Leaving two terms on the right-hand side, one gets the well-known [5] equation of the double-logarithmic approximation which takes into account the most singular components. The next term, with h_1, corresponds to the modified leading-logarithm approximation, and the term with h_2 deals with higher-order corrections. Note that the dependence of γ_0 on y in the integral term has been neglected since it leads to terms of the order of γ_0^2 compared with those written above.

The straightforward solution of Eqn (63) looks very problematic even if the terms with h_1 and h_2 are included in addition just to double-logarithmic ones. However, it is very simple for the moments of the distributions [13] since $G(z)$ and $\ln G(z)$ are the generating functions for the factorial moments and cumulants, respectively. Using formulas (7) and (8) in the case of F scaling, one gets the product $q\gamma$ (and its derivatives) at each differentiation of those functions because the average multiplicity is the only y-dependent term left. The coefficients of z^q on both sides should be equal. Hence, one obtains

$$H_q = \frac{K_q}{F_q} = \frac{\gamma_0^2[1 - 2h_1q\gamma + h_2(q^2\gamma^2 + q\gamma')]}{q^2\gamma^2 + q\gamma'}. \tag{66}$$

The anomalous dimension γ is defined by Eqn (57). The condition $F_1 = K_1 = 1$ determines the relation between γ and γ_0:

$$\gamma \approx \gamma_0 - \frac{1}{2}h_1\gamma_0^2 + \frac{1}{8}(4h_2 - h_1^2)\gamma_0^3 + \mathrm{O}(\gamma_0^4), \tag{67}$$

which shows that the increase of the average multiplicity with energy is slower in the modified leading-logarithm approximation as compared with the double-logarithmic approximation because the term with h_1 is negative [see Eqn (57)]. However, the higher-order terms slightly enlarge it again ($4h_2 - h_1^2 > 0$) but those corrections are not large. The running property of γ_0 has been taken into account in expression (67):

$$\gamma_0' \approx -h_1\gamma_0^3 + \mathrm{O}(\gamma_0^5) \,, \tag{68}$$

which leads to

$$\gamma' \approx -h_1\gamma_0^3(1 - h_1\gamma_0) + \mathrm{O}(\gamma_0^5) \,. \tag{69}$$

The lesson we learn from Eqn (66) is that in all 'correction' terms (which contain h_1, h_2, ...) the expansion parameter γ appears in the product of rank $q\gamma$, which becomes large at high ranks, i.e. at high multiplicities. Therefore, for high multiplicity events one should take into account the ever-higher-order terms in γ. This problem was mentioned a long time ago [5] and discussed in some detail in Ref. [38], but has only recently been analysed.

As was mentioned, the double-logarithmic formulas are obtained from Eqn (63) for $h_1 = h_2 = 0$, $\gamma = \gamma_0$, and $\gamma' = 0$. In this case,

$$H_q \sim q^{-2} \,, \tag{70}$$

which is similar to the asymptotics of the negative binomial distribution with a rather small value of the parameter $k \approx 2$ and corresponds to an extremely wide multiplicity distribution [see expression (23)] while experimental data provide values of k ranging from 3.5 to $\sim$100.

Perhaps a more interesting feature is the evolution of the qualitative behaviour of the ratio H_q at higher orders. In the modified leading-logarithm approximation in which the h_1 term has been kept but the h_2 term (as well as higher-order terms) neglected in Eqn (63), we observe that H_q crosses the abscissa, acquires a minimum at

$$q_{\min} \approx \frac{1}{h_1\gamma_0} + \frac{1}{2} \approx 5 \tag{71}$$

and tends to zero from below as $\sim -q^{-1}$. If one includes the term with h_2 as well, the ratio H_q gets the second zero and tends asymptotically to a positive constant $h_2\gamma_0^2$. This is similar to the situation of the expansion of, for example, $\cos x$ in a Taylor series. That is why it is no surprise that one gets an oscillating behaviour of H_q [39] when account is taken of the higher-order terms with h_3 and h_{11} in formula (63). The very first minimum reveals just the first oscillation, as shown in Fig. 6. However, it has been shifted to $q \approx 4$ in the approximation of Ref. [39], which shows a high sensitivity of H_q to various assumptions. Let us emphasise that the amplitudes of extrema and the periodicity of 'quasioscillations' are different from all those shown in Figs 1–4. The analogous behaviour of H_q has been found as the exact solution of the QCD equations for fixed coupling constant (see Section 7.2).

Figure 6. The ratio H_q as a function of q [39] reveals 'quasi-oscillations' in higher-order perturbative QCD (the curve is drawn for energies of Z^0). The first minimum is slightly shifted (compared with gluodynamics) to $q = 4$.

Thus, we have demonstrated in this section that the conservation laws and other higher-order terms lead, in the framework of gluodynamics, to a substantial reduction of the width of the multiplicity distribution and to a qualitative change of the behaviour of the cumulant and factorial moments.

6. Approximate solutions of QCD equations with running coupling constant

The transition from gluodynamics to QCD, in which quarks are created beside gluons, leads back to the system of the two coupled equations (50) and (51) for the generating functions of quarks and gluons instead of to the single equation (56). Their structure, however, does not differ, in principle, from the gluodynamics equation described in detail above. That is why I shall not write down all the relations (see e.g. [32, 40, 41]), and describe just the results obtained.

In complete analogy to gluodynamics, one gets the system of the coupled recurrent equations for factorial moments and cumulants when the Taylor series expansion is used. This has been solved numerically [40]. The properties of gluon jets do not change noticeably, i.e. their cumulants and factorial moments are very close to those calculated in gluodynamics. The gluon ratio H_q has its minimum at the same value $q \approx 4$ or 5. The quark factorial moments are larger than those of gluon jets, i.e. the parton multiplicity distribution for quark jets is wider than that for gluon jets even though the average multiplicity is smaller there. The first minimum of quark cumulants and of their ratio to factorial moments is located at $q \approx 8$.

To apply these results to the real process of the electron–positron annihilation, one should relate its generating function to those for quark and gluon jets. Bearing in mind the Feynman diagram for the production of two quark jets at the very early stage, one would write down

$$G_{e^+e^-} \approx G_F^2 \,, \tag{72}$$

with further corrections (see e.g. Ref. [32]). In that case the zeros of the quark jet cumulants and of e^+e^- processes coincide because the logarithms of the generating functions which determine corresponding cumulants [see Eqn (5)] are proportional to one another. It means that the first minimum for e^+e^- would lie at $q \geqslant 6$ since the first zero for quark jets is positioned at $q > 5$. The analysis of experimental data described below (see Section 8) points out that this is not the case and either relation (72) should be revised or the higher-order terms in the Taylor series expansion become crucial. The latter possibility appears less probable because the similar shift of the zeros of the quark cumulants has been observed in the case of the exact solution with fixed coupling, as described in the next section. Independently of this, it seems that the most important conclusion drawn from the theoretical studies is

the presence of maxima and minima of the ratio H_q which replace each other with some periodicity (but not at neighbouring values of q as happens for fixed multiplicity).

It is interesting to note that the equations for the low-order moments give rise to conclusions about the anomalous dimension γ and about the ratio $r = \langle n_G \rangle / \langle n_F \rangle$ of the average multiplicities in gluon and quark jets [41]. They have been represented by the perturbative expansion as

$$\gamma = \gamma_0(1 - a_1\gamma_0 - a_2\gamma_0^2) , \tag{73}$$

$$r = \frac{N_c}{C_F}(1 - r_1\gamma_0 - r_2\gamma_0^2) . \tag{74}$$

The coefficients a_i, r_i have been calculated [41] and are shown in Table 1 together with values of r and γ_0 for various numbers of flavours. Fig. 7 demonstrates the Q-dependence of γ resulting from the solution of the equations in the higher-order approximation discussed above. The corresponding behaviour of the average multiplicity is shown in Fig. 8. For comparison, the energy (y) dependence of the mean multiplicity for fixed coupling constant is indicated by dotted lines. To begin with it increases rather slowly but at higher energies its asymptotic increase exceeds that of the running coupling case. This is reliable since the constant has been chosen at rather high energy (mass of Z^0) at $y_{Z^0} = 6.67$, i.e. its value is quite small. In the real situation, it should increase during the evolution of the jet, but the number of active flavours must decrease. Let us note that these two trends somewhat compensate one another in the energy dependence of the mean multiplicity. The ratio r of the mean multiplicities in gluon and quark jets is much smaller [41] than its value in the double-logarithmic approximation where it is equal to $\frac{9}{4}$. On average, it is lower by about 20%. The analogous situation is for exact solutions of equations with fixed coupling constant. Therefore, that ratio is considered in more detail in the next section.

Table 1.

n_f	r	r_1	r_2	γ_0	a_1	a_2
3	1.84	0.185	0.426	0.473	0.280	−0.379
4	1.80	0.191	0.468	0.481	0.297	−0.339
5	1.77	0.198	0.510	0.484	0.314	−0.301

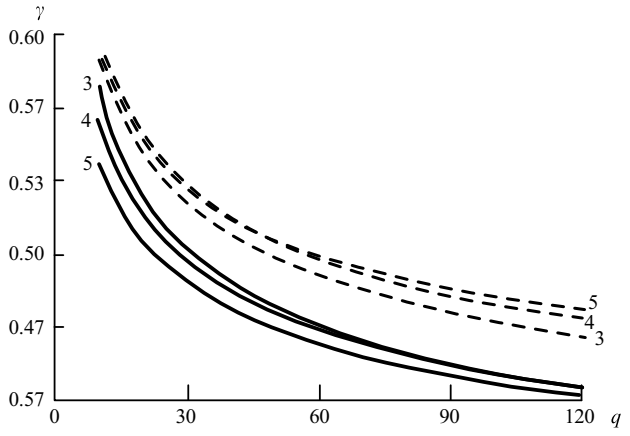

Figure 7. q dependence of the anomalous dimension γ [41] (solid lines) in the case of the running coupling γ_0 (dashed lines) for different numbers (indicated near the lines) of active flavours.

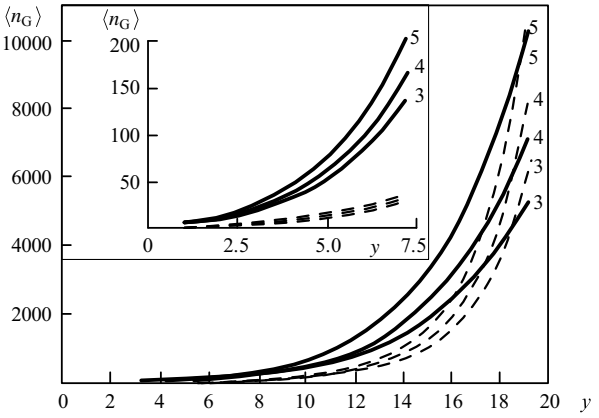

Figure 8. y dependence of the average multiplicity for running (solid lines) and fixed (dashed lines) coupling [41] with the number of active flavours $n_f = 3, 4, 5$. The arrow marks the y_{Z^0} location.

7. Exact solutions of QCD equations with fixed coupling constant

The above experience with QCD equations treated in various approximations suggests that the conservation laws and nonsingular terms of the kernels play a more important role than the dependence of the coupling constant on the evolution parameter. It can be shown [21, 42] that the equations (50) and (51) can be solved exactly if the coupling constant is fixed. No other assumptions are necessary. One obtains the general solution for the moments of any rank but we start with the lowest ranks for pedagogical reasons.

7.1 First moments and the ratio of average multiplicities in gluon jets to those in quark jets

The equations for average multiplicities (unnormalised moments of first order) are derived from the system of equations (50) and (51) if one substitutes the generating functions as series (7) and equates the terms linear in z with the conditions $F_0 = F_1 = \Phi_0 = \Phi_1 = 1$. (The factorial moments of quark jets are denoted by Φ_q and their cumulants are denoted by Ψ_q.) If the coupling constant is kept fixed, the average multiplicities behave [5] as

$$\langle n_G(y) \rangle = \exp(\gamma y) , \quad \langle n_F(y) \rangle = \exp(\gamma y)\, r^{-1} , \tag{75}$$

where the anomalous dimension γ and the ratio r are constant. These properties are inherited in equations (50) and (51) as one notices from the relations

$$\frac{\langle n_{G,F}(y + \ln x) \rangle}{\langle n_{G,F}(y) \rangle} = x^{\gamma} , \tag{76}$$

$$\langle n_{G,F}(y) \rangle' = \gamma \langle n_{G,F}(y) \rangle . \tag{77}$$

Then the equations are rewritten as a system of two algebraic equations for two variables γ and r:

$$\gamma = \gamma_0^2[M_1^G + n_f r(M_1^F - M_0^F)] , \tag{78}$$

$$\gamma = \gamma_0^2(L_2 - L_0 + rL_1) , \tag{79}$$

where

$$M_1^{\mathrm{G}} = \int_0^1 \mathrm{d}x\, K_{\mathrm{G}}^{\mathrm{G}}[x^\gamma + (1-x)^\gamma - 1] ,$$

$$M_1^{\mathrm{F}} = \int_0^1 \mathrm{d}x\, K_{\mathrm{G}}^{\mathrm{F}}[x^\gamma + (1-x)^\gamma] ,$$

$$M_0^{\mathrm{F}} = \int_0^1 \mathrm{d}x\, K_{\mathrm{G}}^{\mathrm{F}} = \frac{1}{2} M_1^{\mathrm{F}}(\gamma = 0) ,$$

$$L_1 = \int_0^1 \mathrm{d}x\, K_{\mathrm{F}}^{\mathrm{G}} x^\gamma ,$$

$$L_2 = \int_0^1 \mathrm{d}x\, K_{\mathrm{F}}^{\mathrm{G}} (1-x)^\gamma ,$$

$$L_0 = \int_0^1 \mathrm{d}x\, K_{\mathrm{F}}^{\mathrm{G}} = L_1(\gamma = 0) .$$

Coefficients M_i and L_i can be expressed in terms of Euler beta-functions and psi-functions and depend on γ only. At fixed γ_0, both γ and r are constant. It should be stressed that γ is not equal to γ_0 even in gluodynamics at $n_{\mathrm{f}} = 0$ because M_1^{G} differs from γ^{-1}. The approximate equality is valid for $\gamma_0 \ll 1$ but the perturbative expansion for γ differs from the corresponding formula (67) for the running coupling constant

$$\gamma \approx \gamma_0 - h_1\gamma_0^2 + \tfrac{1}{2}(h_1^2 + h_2)\gamma_0^3 + \mathrm{O}(\gamma_0^4) , \tag{80}$$

from which one sees that the first correction is twice as large.

The ratio r appears in equations (78) and (79) linearly, and one is tempted to rewrite them as

$$r(\gamma) = b(\gamma)\left[\frac{\gamma}{\gamma_0^2} - a(\gamma)\right]^{-1} , \tag{81}$$

$$r(\gamma) = \left[\frac{\gamma}{\gamma_0^2} - d(\gamma)\right]\frac{1}{c(\gamma)} , \tag{82}$$

where

$$a = \psi(1) - \psi(\gamma+1) + B(\gamma,1) - 2B(\gamma+1,2) - 2B(\gamma+2,1) + B(\gamma+2,3) + B(\gamma+3,2) + \frac{11}{12} - \frac{n_{\mathrm{f}}}{6N_{\mathrm{c}}} ,$$

$$b = \frac{n_{\mathrm{f}}}{2N_{\mathrm{c}}}[B(\gamma+3,1) + B(\gamma+1,3)] ,$$

$$c = \frac{C_{\mathrm{F}}}{N_{\mathrm{c}}}[B(\gamma,1) - B(\gamma+1,1) + \frac{1}{2}B(\gamma+2,1)] ,$$

$$d = \frac{C_{\mathrm{F}}}{N_{\mathrm{c}}}\left[\psi(1) - \psi(\gamma+1) - B(\gamma+1,1) + \frac{1}{2}B(\gamma+1,2) + \frac{3}{4}\right] .$$

All beta-functions are just the inverse polynomials of γ but the above notation is less cumbersome. The solution of the algebraic relations (81) and (82) yields γ and r as functions of γ_0 and n_{f}. Fig. 9 shows the dependence of γ on γ_0 for $n_{\mathrm{f}} = 3, 4, 5$. The differences for the various values of n_{f} are hardly discernable, being less than the thickness of the visible line. Note that γ is significantly different from γ_0. They can be related by the simple fitted formula

$$\gamma = 0.077 + 0.62\gamma_0 , \tag{83}$$

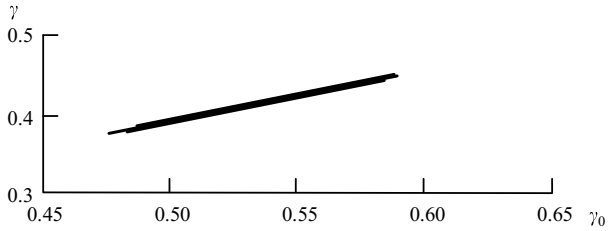

Figure 9. γ plotted as a function of γ_0 for $n_{\mathrm{f}} = 3, 4, 5$ [42].

or by the more theoretically motivated formula (80) starting from the linear terms in γ_0,

$$\gamma = 0.97\gamma_0 - 0.48\gamma_0^2 + 0.2\gamma_0^3 , \tag{84}$$

fitted by computer in the range of γ_0 from 0.48 to 0.6. Let us note that γ changes very slowly with γ_0. In itself, the value of γ is not of much interest even though it is related to the energy dependence of the average multiplicity. However, it is known that the power increase of the mean multiplicity for fixed coupling is replaced by a slower dependence for running coupling [see Fig. 8]. Somehow the reduced value of γ compared with γ_0 respects that tendency but the dependence (75) cannot be used in asymptotics. The more realistic behaviour provided by the running coupling was discussed in the previous section (see Fig. 8).

The corresponding ratio r is of more interest since the energy dependences of the average multiplicities in gluon and quark jets cancel. That is why its prediction for fixed coupling could be more general. The corresponding result on the ratio r is shown in Fig. 10. Again the dependence on n_{f} is very mild, and is exhibited in the expanded scale in Fig. 10. More important, the dependence of r on γ_0 is even weaker than that of γ, and the average effective value is given by

$$r = 1.84 \pm 0.02 . \tag{85}$$

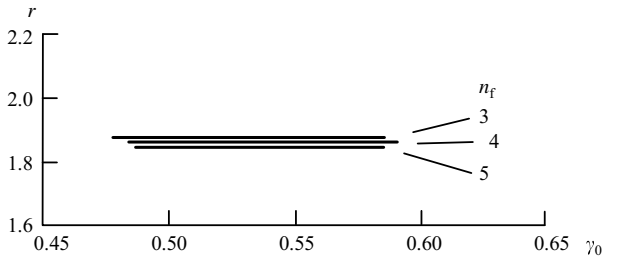

Figure 10. r plotted as a function of γ_0 for $n_{\mathrm{f}} = 3, 4, 5$ [42].

Such a low value of the ratio r should arouse interest since, in the double-logarithmic approximation, it is much larger [5] and equal to $N_{\mathrm{C}}/C_{\mathrm{F}} = \frac{9}{4}$. It has been reduced to 2.05 in the modified leading-logarithm approximation [43, 44]. The above value shows that the conservation laws diminish the ratio further. Even lower values of r have been obtained for running coupling (see [41] and Table 1).

In a realistic process, the virtuality in a jet degrades as partons evolve toward hadrons, presumably with an associated change in the number of active quark flavours. In the framework of our calculations with fixed

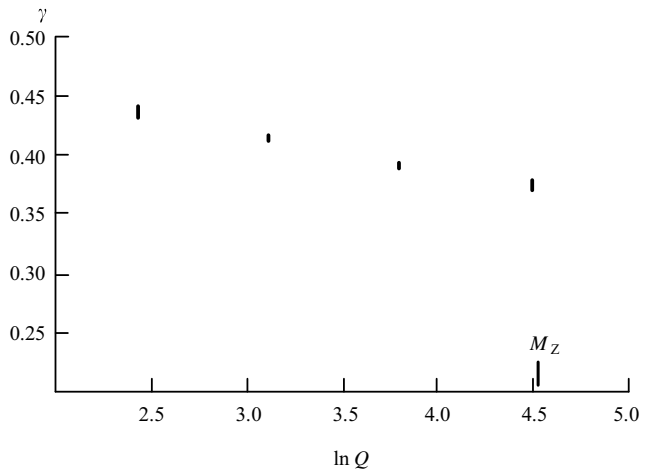

Figure 11. γ plotted as a function of $\ln Q$ for $n_f = 3, 4, 5$ and $Q = M_Z/m$ [42] ($m = 1, 2, 4, 8$).

coupling, this dependence can be considered with the aid of the formulas

$$\gamma_0^2 = \frac{12}{\beta_0 y}, \quad \beta_0 = 11 - \frac{2n_f}{3}, \tag{86}$$

for $y = \ln Q/Q_0, Q_0 = 0.65/\Lambda_{\overline{MS}}$, where the dependence of $\Lambda_{\overline{MS}}$ on n_f is included according to the proportions $63:100:130$ for $n_f = 5:4:3$, respectively [45], and the value $\Lambda_{\overline{MS}}$ is set at 175 MeV for $n_f = 5$. The values of Q are considered at M_Z/m (M_Z being the mass of Z^0) for $m = 1$, 2, 4, and 8. The result on γ is shown as a function of $\ln Q$ in Fig. 11. The dependence on n_f is so small that connection of the different points with different n_f for the same Q results in only short line segments as shown. Thus, we learn that as a jet of partons evolves toward lower Q, we need not be concerned with the change of the active flavour, and that the parton multiplicity will depend on the evolving virtuality through a mild variation of γ, but not enough to invalidate fixed coupling approximation. Certainly, in the ratio of the multiplicities, such dependences are cancelled, yielding a stable value of r. This conclusion has been supported by the approximate solutions of the equations with the running coupling [41], as has already been discussed already (see Table 1).

7.2 Higher-order moments and widths of distributions in gluon and quark jets

The dispersion of the multiplicity distribution is determined by the second moment. Therefore, to get it one should solve the system of equations (50) and (51) for $q = 2$. However, relations (76) and (77) prompt us to obtain the solution for any q. In fact, one can obtain a system of coupled recurrent equations [21] for moments if one substitutes in Eqns (50) and (51) the generating functions according to Eqn (7) and compares the coefficients of z^q on both sides. Those equations are solved by iteration, which is well suited for computer calculations. They will not be written down here (see [21]); just the final analytic expressions for the moments of rank q as related to the lower rank moments will be given. For that purpose, let us introduce

$$f_q = \frac{F_q}{q!}, \quad \hat{\phi}_q = \frac{\Phi_q}{r^q q!}. \tag{87}$$

The solution of the equation is [21]

$$f_q = [a_q S_q(f, \hat{\phi}) + b_q T_q(f, \hat{\phi})]\Delta_q^{-1}, \tag{88}$$

$$\hat{\phi}_q = [c_q S_q(f, \hat{\phi}) + d_q T_q(f, \hat{\phi})]\Delta_q^{-1}, \tag{89}$$

where

$$S_q = \sum_{l=1}^{q-1}\left(N^G_{q,l} f_l f_{q-l} + n_f N^F_{q,l}\hat{\phi}_l\hat{\phi}_{q-l}\right), \tag{90}$$

$$T_q = \sum_{l=1}^{q-1} L_{q,l}\hat{\phi}_l f_{q-l}, \tag{91}$$

$$a_q = \frac{q\gamma}{\gamma_0^2} + L_{0,0} - L_{q,q}, \tag{92}$$

$$b_q = n_f M^F_q, \tag{93}$$

$$c_q = L_{q,0}, \tag{94}$$

$$d_q = \frac{q\gamma}{\gamma_0^2} - M^G_q + n_f N^F_{0,0}, \tag{95}$$

$$\Delta_q = a_q d_q - b_q c_q, \tag{96}$$

$$M^G_q = \psi(1) - \psi(q\gamma+1) + B(q\gamma, 1) - 2B(q\gamma+1, 2)$$

$$-2B(q\gamma+2, 1) + B(q\gamma+2, 3) + B(q\gamma+3, 2) + \frac{11}{12},$$

$$M^F_q = \frac{1}{2N_c}[B(q\gamma+3, 1) + B(q\gamma+1, 3)],$$

$$N^G_{q,l} = B[l\gamma, (q-l)\gamma+1] - 2B[l\gamma+1, (q-l)\gamma+2] + B[l\gamma+2, (q-l)\gamma+3],$$

$$N^F_{q,l} = \frac{1}{4N_c}\{B[l\gamma+3, (q-l)\gamma+1] + B[l\gamma+1, (q-l)\gamma+3]\},$$

$$L_{q,l} = \frac{C_F}{N_c}\{B[l\gamma+1, (q-l)\gamma] - B[l\gamma+1, (q-l)\gamma+1] + \frac{1}{2}B[l\gamma+1, (q-l)\gamma+2]\}.$$

The above expressions look cumbersome† but their structure is very simple and clear. They generalise the formulas of the preceding section to any q. The formulas of gluodynamics follow from those for $n_f = C_F = 0$ if one leaves in M^G_q and $N^G_{q,l}$, the leading terms $B(q\gamma, 1) \equiv 1/q\gamma$, and $B[l\gamma, (q-l)\gamma+1]$. Using the values of γ and r from the preceding section at given γ_0 and n_f, one obtains first F_2 and Φ_2, and then increases q by 1.

The evolution parameter y disappears from the formulas. A posteriori, it means that our assumption about F scaling with all dependence on y hidden in the average multiplicities $\langle n_{G,F}\rangle(y)$ is correct for fixed coupling. It leads to the self-consistent system of algebraic equations where all quantities, including F_q and Φ_q, are independent of energy. It should be stressed that F scaling is as precise as the main equations at fixed coupling. In fact, one should speak about asymptotic F scaling because the limits of x-integration in Eqns (50) and (51) are asymptotic. More precise treatment of them would correspond to considering the higher twist effects.

†The gluodynamics formulas are obtained from them in the limit $n_f = C_F = 0$ when only the leading terms of M_q and of $N^G_{q,l}$ are considered, i.e. $B(q\gamma, 1) \equiv 1/q\gamma$ and $B[l\gamma, (q-l)\gamma+1]$.

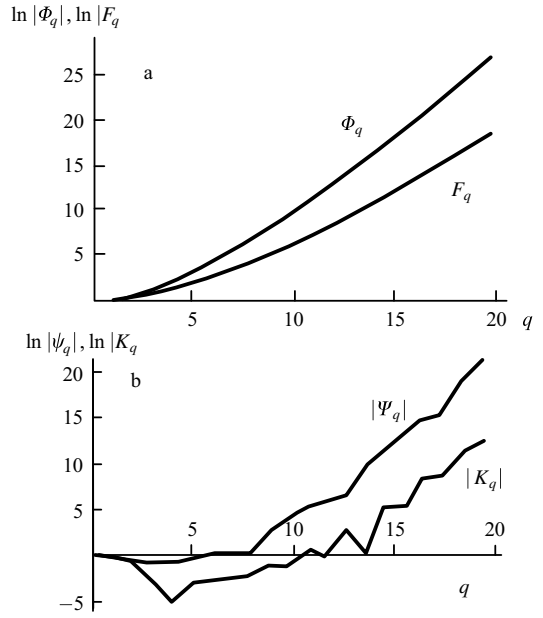

Figure 12. Moments of multiplicity distribution in fixed-coupling QCD for $\gamma_0 = 0.48$, $n_f = 5$ [21]. (a) $\ln F_q$, $\ln \Phi_q$, (b) $\ln |K_q|$, $\ln |\Psi_q|$.

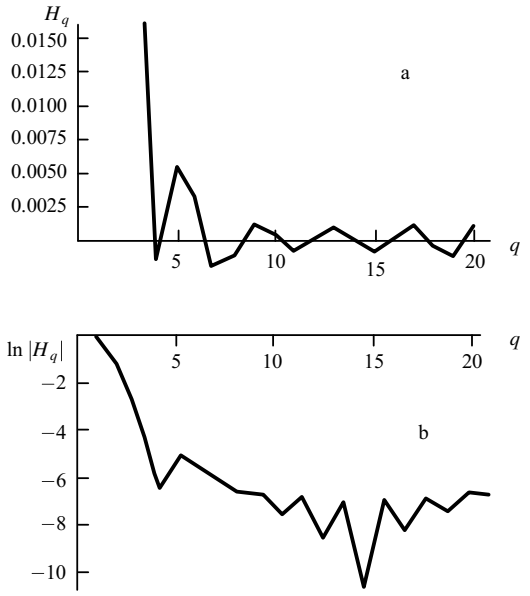

Figure 13. Ratio H_q of gluon-jet distribution in fixed-coupling QCD for $\gamma_0 = 0.48$, $n_f = 5$ [21]. (a) H_q, (b) $\ln |H_q|$.

The results of calculation, when expressed in terms of F_q and Φ_q, are shown in Fig. 12 for $\gamma_0 = 0.48$ and $n_f = 5$. Evidently, they increase rapidly with q, more so for Φ_q than for F_q. Since these are normalised factorial moments, they imply that the multiplicity distribution for the quark jet is wider than that for the gluon jet, although the average multiplicity in quark jets is lower than in gluon jets. These results are very insensitive to the number of active flavours n_f. The dependence on the coupling constant is very mild and the results are rather insensitive to the coupling constant being fixed or running.

Let us compare the QCD results to those of the phenomenological distributions. By comparison of Fig. 12 with Fig. 2 and Fig. 3, the QCD results are clearly of the NBD type rather than the fixed multiplicity type. In fact, F_q in Fig. 12 can be approximated by a negative binomial distribution with $k = 5$. However, this is an apparent coincidence. While the characterisation of F_q by the NBD parameter k is convenient, the fits by the negative binomial distribution are inappropriate. Let us recall that the cumulants of the negative binomial distribution decrease at low q and then increase. The ratio H_q decreases monotonically with q.

The corresponding ratios for gluon and quark jets are defined here as:

$$H_q = \frac{K_q}{F_q}, \tag{97}$$

$$\eta_q = \frac{\Psi_q}{\Phi_q}, \tag{98}$$

where $K_q(\Psi_q)$ are related to $F_q(\Phi_q)$ by formula (11). The results of calculations in fixed-coupling QCD are shown in Figs 13 and 14.

The distinctive feature of the behaviour of H_q is clearly its oscillations. There are no oscillations for the negative binomial distribution even if it fits the second and third moments quite well. One sees that the fixed multiplicity

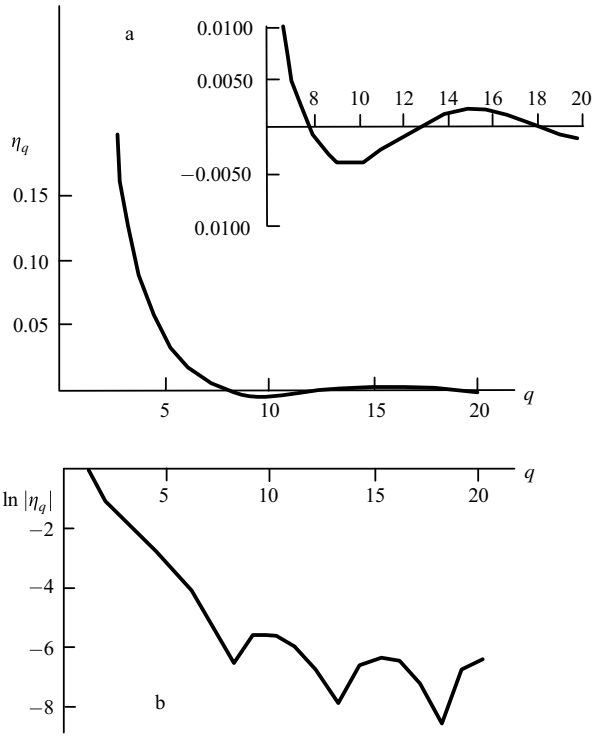

Figure 14. Ratio η_q of quark-jet distribution in fixed-coupling QCD for $\gamma_0 = 0.48$, $n_f = 5$ [21]. (a) η_q, (b) $\ln |\eta_q|$.

distribution, which gives rise to oscillations of H_q changing sign at each subsequent integer value of q, does not suit us because of the wrong values of moments and the improper period of oscillations (see the discussion of experimental results in the following section).

The sensitivity of H_q to the shapes of the distributions obtained in QCD with different assumptions is clearly demonstrated by its various qualitative forms. It is positive

and decreases monotonically as $\sim q^{-2}$ in the double-logarithmic approximation, acquires a zero and a minimum in the modified leading-logarithm approximation tending asymptotically to zero from below like $\sim -q^{-1}$, acquires a second zero and constant positive asymptotics because of the next term, and starts oscillating in the higher-order approximations.

The behaviour of H_q depends strongly on slight variations of the particular shape of factorial moments at low values of q. One can demonstrate how easy it is to obtain oscillations of the fixed multiplicity type imposed on the double-logarithmic behaviour by doing the following exercise. It is known [19, 46] that the large q behaviour of F_q of the factorial moments in the double-logarithmic approximation [see Eqn (23)] is

$$F_q = \frac{2q\Gamma(q+1)}{C^q}\,. \tag{99}$$

If one adds a preasymptotic term by replacing the factor $2q$ by $2q+1$ in the numerator (which restores the condition $F_0 = 1$ but not $F_1 = 1$), one gets an additional term in H_q which imposes oscillations of the fixed multiplicity type on the monotonic decrease of the form q^{-2}, and the ratio H_q becomes

$$H_q = \frac{2 + (-1)^{q-1}}{q(2q+1)}\,, \tag{100}$$

where the second term in the numerator appears because of the newly added preasymptotic term.

The above examples show how sensitive H_q is to various approximations made in solving the set of equations for the generating functions. Their distinction has been demonstrated in Figs 4, 6, 13, and 14, and they strongly differ from the phenomenological distributions shown in Figs 2 and 3. Unfortunately, there is still no clear understanding of the physical origin of the oscillations, i.e. of their periodicity, amplitude, and dependence on the rank q (it seems that the amplitude increases and the period decreases with q). Nevertheless, the exact solution of fixed-coupling QCD equations provides a clear guide to the realistic behaviour of H_q. Perhaps the behaviour of H_q will show us ways to generalise the equations for the generating functions, including the fine effects of the interaction of 'colour monsters' [5, 19, 46].

Note that the above oscillations proceed at integer values of q and are not related to the oscillation of the fractional moments. The latter would impose the lower-period harmonics on those oscillations.

8. Experiment

Thus, we have obtained the results for the KNO function $f(x)$, for the moments of the multiplicity distribution K_q and F_q, and for their ratio H_q, as well as for the energy behaviour of mean multiplicities (the anomalous QCD dimension γ) and for the ratio r of the average multiplicities in gluon and quark jets. Before comparing them with experiment one should remember that all the above results have been obtained for the multiplicity distributions of partons (gluons and quarks) while experimentalists have to deal with hadrons. To translate theoretical predictions to experimentally measured values, one must construct a hadronisation model describing the transition from partons to hadrons. Then, one can obtain quantitative results using Monte Carlo calculations. SomeTimes, one relies on the hypothesis of the local parton–hadron duality. This assumes that the distributions of partons and hadrons differ by only a numerical coefficient which is determined by the number of partons recombined in a single hadron. Therefore, this is of less importance for the normalised variables, and the normalised moments of gluon and quark jets should simply be related to the moments of observed processes, e.g. to electron–positron annihilation. On the other hand, such values as the average multiplicities in gluon and quark jets are changed in a different way that can vary their ratio also. In this case one could use various Monte Carlo versions of hadronisation. One of them, the Herwig method [47], has been discussed in Ref. [48] in relation to the ratio of the average multiplicities r [Eqn (75)] both on parton and on hadron levels (see Fig. 15). The method supports the asymptotic local parton–hadron duality but does not respect it at intermediate energies in an exact way. The partonic ratio is given by to $r^{\mathrm{MC}}_{\mathrm{parton}} \approx 1.9$. It shows that the higher-order corrections play an important role in the Herwig approach because this value is smaller than those of the lowest-order approximations as discussed above. The hadronic ratio is slightly lower in asymptotics. However, it is still much lower at energies of Z^0 (equal to 1.44) and increases with energy. This indicates that the local parton–hadron duality is not yet very accurate. The model describes the bulk of experimental data even though it admits slight revisions. In particular, if one modifies the partonic cascade so that it gives rise to a value of the partonic ratio obtained above $r_{\mathrm{theor}} = 1.84 \pm 0.02$ [Eqn (85)] and considers the same hadronisation model to deal with the same ratio of hadrons to partons $r^{\mathrm{MC}}_{\mathrm{hadron}}/r^{\mathrm{MC}}_{\mathrm{parton}} = 1.44/1.92$ (see Fig. 15), i.e. applies the formula

$$r_{\mathrm{exp}} = r_{\mathrm{theor}}\left(\frac{r^{\mathrm{MC}}_{\mathrm{hadron}}}{r^{\mathrm{MC}}_{\mathrm{parton}}}\right)\,, \tag{101}$$

one obtains

$$r_{\mathrm{exp}} \approx 1.38 \pm 0.02\,, \tag{102}$$

which agrees quite well with the recently measured [49] value $1.27 \pm 0.04 \pm 0.06$ (see also Ref. [50]). Therefore, we can state that there is no longer a disagreement between

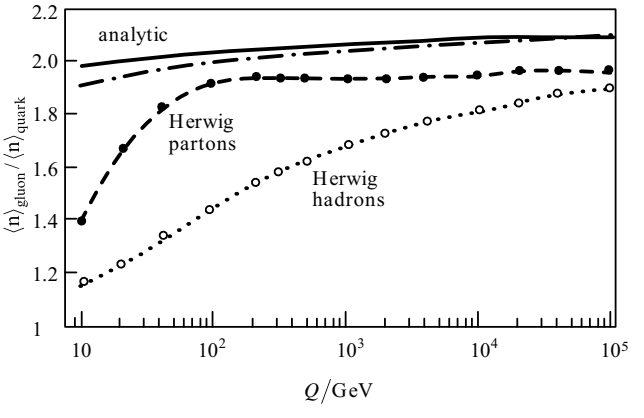

Figure 15. Ratio r of average multiplicities in gluon and quark jets [48]. Analytic results are shown by the upper curves. Results obtained from the Herwig Monte Carlo method at the parton and hadron levels are also shown.

theoretical and experimental values of the ratio of average multiplicities in gluon and quark jets. Still, one should keep in mind that the phenomenologically described hadronisation plays an important role in reducing this value by 40% when going from partonic to hadronic levels.

The KNO function $f(x)$ becomes narrower when energy conservation is taken into account in a proper way, in contrast to the double-logarithmic approximation, as was discussed in Section 5.1. The negative binomial distribution fits it rather well with $k \approx 7$, as is seen from Fig. 5. The Monte Carlo calculations fit experiment as well. However, it should be stressed once again that some tiny features escape such a comparison, as revealed when studying the behaviour of the ratio of cumulant to factorial moments H_q.

These ratios differ for gluon and quark jets as shown in Figs 13 and 14. Therefore, they may be used either for selection of those jets, or for the control of the validity of their separation performed according to other criteria (see e.g. Refs [49, 50]). The qualitative characteristics of the curves are hardly changed by hadronisation Monte Carlo calculations, but this is yet to be confirmed.

The transition from generating functions of jets to real processes of hadroproduction is nontrivial even for e^+e^- annihilation as has been discussed above, and much more complicated for other processes. Hopefully the qualitative features of jet moments are more general. Then it would be reasonable to compare them with the corresponding characteristics of multiparticle production processes in an attempt to reveal their interrelation and, in particular, the role of hadronisation.

Such an analysis has been performed [51] both for e^+e^- annihilation and for pp (and $p\bar{p}$) interactions in a wide energy interval to get some idea of the difference between the processes initiated by leptons and by hadrons. A list of the samples of experimental data [52–56] considered is given in Table 2. Small statistical samples, yielding large error bars, have been disregarded, and only papers reporting a detailed separation between elastic and inelastic

Table 2. Investigated data.

Interaction	Experiment, spectrometer, or collaboration name	CMS energy or beam moment	No. of events
e^+e^-	TASSO [52]	22 GeV	1913
	HRS [53]	29	29649
	TASSO [52]	34.8	52832
	TASSO [52]	43.6	8620
	ALEPH [54]	91	90000
	DELPHI [55]	91	47400
	L3 [56]	91	169700
	OPAL [57]	91	82941
pp	FNAL [61]	300 GeV/c, $\sqrt{s}$ = 23.8 GeV	8477
	SMF detector at CERN [63]	30.4	37069
	E743 FNAL [62]	800 GeV/c, $\sqrt{s}$ = 38.8	10217
	SMF detector at CERN [63]	52.6	26842
	SMF detector at CERN [63]	62.2	58196
	UA5 [64]	200	4156
	UA5 [65]	546	7775
	UA5 [64]	900	6839

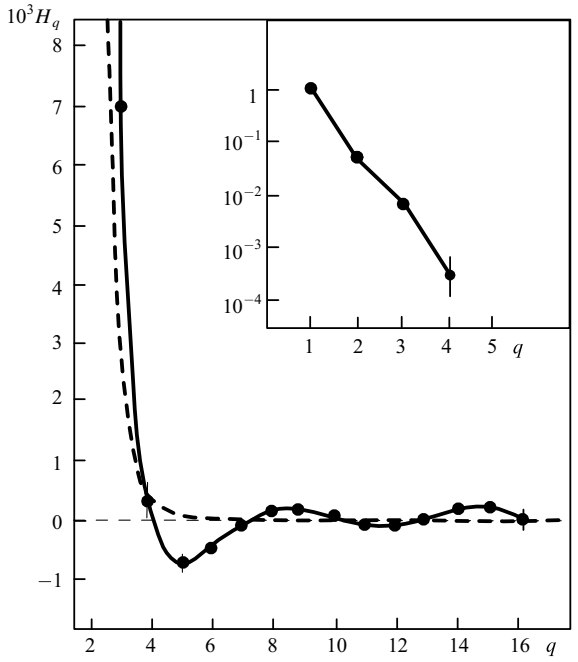

Figure 16. H_q plotted as a function of q in the e^+e^- data of DELPHI collaboration at 91 GeV [51].

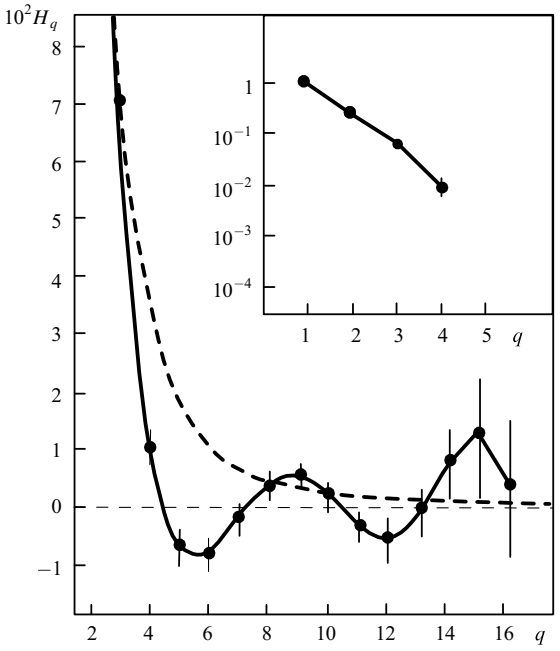

Figure 17. H_q plotted as a function of q in the $p\bar{p}$ data of UA5 collaboration at 546 GeV [51].

data for low multiplicities have been taken into account. For all the considered experimental multiplicity distributions of secondary hadrons the ratio H_q has been computed up to the 16th order. In fact, the qualitative features of the behaviour of H_q are very similar in all processes, though the detailed structure depends on the type of interaction, on the energy, and even on the experimental sampling of events.

As a first example one may consider the outcomes of the e^+e^- 91 GeV DELPHI multiplicity distribution [55] plotted in Fig. 16. Owing to the different order of magnitude

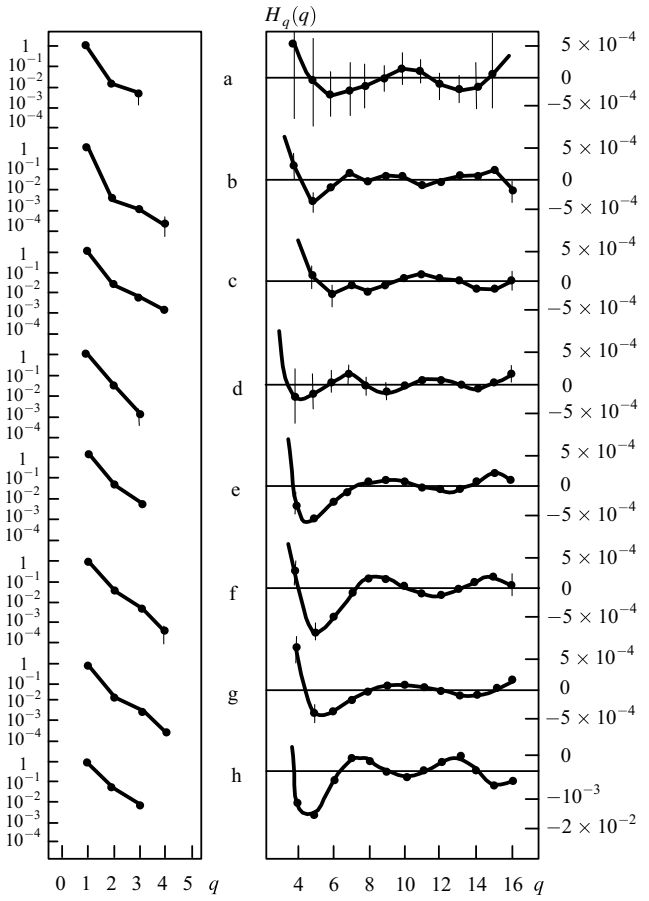

Figure 18. H_q plotted as a function of q in e^+e^- data in a wide energy interval [51] (experimental groups are ordered as in Table 2, i.e. the energy increases from top to bottom). On the left the lowest orders are shown in the log scale, on the right the higher orders in the linear scale.

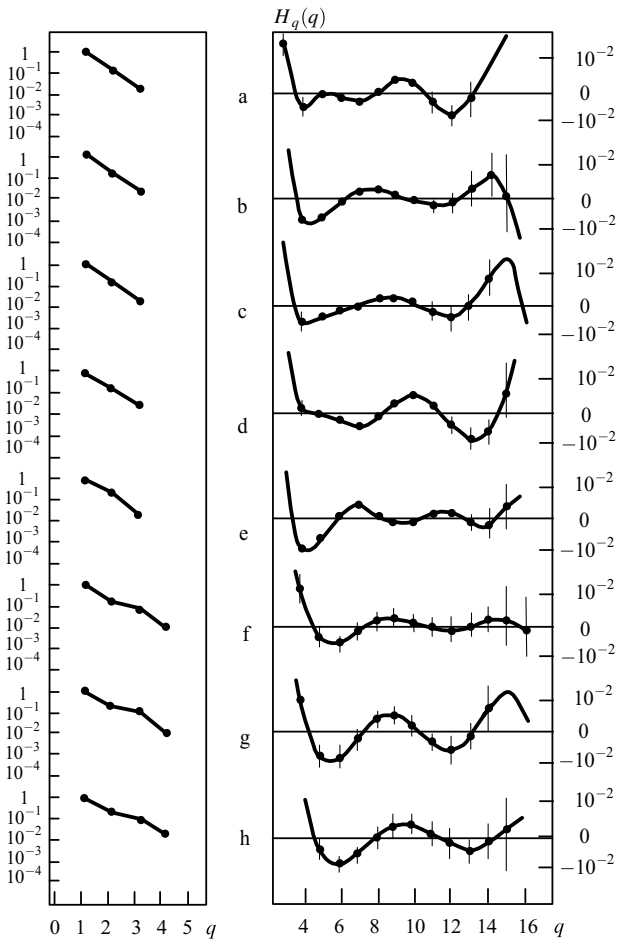

Figure 19. H_q plotted as a function of q in pp (and $\bar{p}p$) data in a wide energy interval [51] (the comments are the same as in Fig. 18).

involved here, the low-q and high-q regions are plotted on different scales. The lines connecting the points in the inset displays, up to the 4th order, the abrupt descent of H_q (the scale is logarithmic). In the main reference frame, two negative minima (at $q \approx 5$ and 12) and two positive maxima (at $q \approx 8$ and 15) are shown. The predictions of the negative binomial distribution are given by the dashed curve shown in Fig. 16. The value of the parameter k has been taken from Ref. [55] ($k^{-1} = 0.0411 \pm 0.0012$). No minima or maxima appear, of course, and it is tempting to conclude that the negative binomial distribution is able to reproduce the main details of experimental data at low q but not its tiny details revealed by oscillations at higher q.

Fig. 17 refers to the $\bar{p}p$ 546 GeV interaction outcomes from the UA5 collaboration [65]. The main difference from the previous case is the order of magnitude of the maxima and minima, whose absolute value is more than ten Times larger. Nonetheless, the same main characteristics found for e^+e^- annihilation, i.e. the abrupt descent and the subsequent oscillations, can be observed (here the minima are at $q \approx 5$ and 12 while the maxima are at $q \approx 8$ and 15). Again superimposed (dashed curve) are the negative bimomial yields, here corresponding to the k parameter given in Ref. [65] ($k = 3.69 \pm 0.09$).

Similar qualitative features have been observed at various energies, as shown in Figs 18 and 19. Note that there is a quantitative distinction between the experimental data of different collaborations for the same e^+e^- process at the same energy 91 GeV (see the four lower graphs in Fig. 18). Perhaps this is related to the selection procedures adopted by various collaborations and to systematic errors. The high sensitivity of the ratio H_q could be exploited, e.g. for optimisa-tion of the selection criteria. To check their influence, the various Monte Carlo schemes have been compared with the data on H_q. ARIADNE, which includes the selection criteria of OPAL, has its data given in Fig. 18g while JETSET, suited for DELPHI, has its data shown in Fig. 18f. Since there is a quantitative difference between those data, one concludes that it stems from the particular details of experiments but not from the general dynamics of the process at the parton level. The general trend survives various systematics.

Note that the distinction between experimental and negative binomial distributions has been observed in papers of UA5 [65], DELPHI [55], and OPAL [57]. The latter collaboration has shown that the difference between the two distributions oscillates. Perhaps this lies at the origin of the oscillations of H_q, as well. Their physical interpretation could be related to the varying number of subjets in e^+e^- annihilation (see e.g. Ref. [31]) or to the number of 'ladder-strings' in hadronic processes (see e.g. Ref. [27]). Oscillation of the cumulants due to dynamical origin imply immediately that the models with Poisson

distributed clusters [28, 84] are inappropriate for the precise description of experimental data.

The more trivial effect of the cut-off of the experimental distributions at large multiplicities could be of importance since it produces some oscillations of H_q also. In distinction to dynamical oscillation of QCD, this effect should, however, vanish at asymptotically high energies. Nevertheless, further study needs to be done.

To conclude, one can say that the QCD predictions have become more reliable at the qualitative level in recent years and have gained support from experimental data on multiplicity distributions. There now exist both the proper approach to the treatment of various theoretical approximations and some proposals for the selection of experimental data for quantitative comparison with theoretical predictions. Therefore, a solid foundation has been laid for the precise description of the problem as a whole.

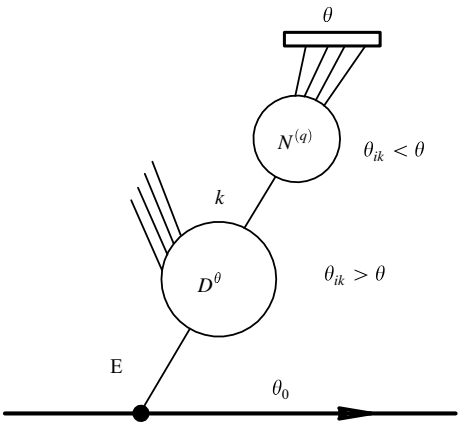

Figure 20. Emission of the gluon (wavy lines) jet by the quark (the solid line) [38].

9. Evolution of distributions with decreasing phase-space volume — intermittency and fractality

The multiplicity distributions can be measured not only in the total phase-space (as has been discussed above for very large phase-space volumes) but in any part of it. For the homogeneous distribution of particles within the volume, the average multiplicity is proportional to the volume and decreases for small volumes but the fluctuations increase. The most interesting problem here is the law governing the growth of the fluctuations, and its possible departure from a purely statistical law related to the decrease of the average multiplicity. Such a variation has to be connected with the dynamics of interactions. In particular, it has been proposed [66] to look for the power-law behaviour of the factorial moments for small rapidity intervals δy

$$F_q \sim (\delta y)^{-\phi(q)} \qquad (\delta y \to 0)\,, \tag{103}$$

where $\phi(q) > 0$. This assumption has been motivated by the analogy to turbulence in hydrodynamics, where the similar property is known as intermittency and $\phi(q)$ are called the intermittency exponents. It originates from the state of the fluid in which the 'quiet' regions alternate with the volumes of high fluctuations, and becomes even more noticeable at smaller sizes. From the point of view of distributions it implies a rather strong increase of their width with slower decline at high multiplicities.

Experimental data on various processes in a wide energy range support the idea by revealing the power-law dependence (103). Immediately, several theoretical approaches were developed to explain that phenomenon. The present state of affairs has been described recently in a review paper [14]. Here, it is just shown how QCD reproduces intermittency [38, 67–71].

Let us stress once again that QCD deals with partons (quarks and gluons) while experimental results provide the moments of distributions of hadrons. The local parton–hadron duality hypothesis implies proportionality of inclusive distributions but is not so obvious for correlations and is not fulfilled someTimes in the proposed Monte Carlo schemes. Therefore, one can pretend to get a qualitative description on the parton level but not attempt a quantitative comparison with experiment.

In contrast to the previous sections, here the diagrammatic approach is relied on instead of the equations for the generating functions. This is because, considering the multiplicity distributions in small phase-space volumes, one has to deal with a minor part of the whole parton content of a well-developed jet; namely, with those partons which fill in the chosen volume. It should be stressed that the prehistory of a jet as a whole is important for the subjet under consideration, as is shown in Fig. 20. Here

(1) the primary quark (solid line) emits a hard gluon with energy E in the direction of the angular interval θ, but not necessarily hitting the window;
(2) the emitted gluon produces a jet of partons with parton splitting angles larger than the window size;
(3) among those partons there exists a parton with energy k which hits the window;
(4) all decay products of the subjet exactly cover the angle θ.

This picture dictates the rules of calculation of the qth correlator of the whole jet. One should average the qth correlator of the subjet $\Delta N^{(q)}(k\theta)$ over all possible ways of its production, i.e. convolute it with the inclusive spectra of such partons D^θ in the whole jet and with the probability of creation of the jet $(\alpha_S K_{\mathrm{F}}^{\mathrm{G}})$. Analytically, this is represented by

$$\Delta N^{(q)}\left(Q\theta_0,\ \frac{\theta_0}{\theta}\right) \propto \int^{Q} \frac{\mathrm{d}E}{E}\frac{\alpha_{\mathrm{S}}}{2\pi} K_{\mathrm{F}}^{\mathrm{G}}\left(\frac{E}{Q}\right) \times \int^{E} \frac{\mathrm{d}k}{k} D^{\theta}\left(\frac{E}{k};\, E\theta_0,\, k\theta\right)\Delta N^{(q)}(k\theta)\,, \tag{104}$$

where $\Delta N^{(q)} \equiv F_q \langle n\rangle^q$ is the unnormalised factorial moment (on the left-hand side for the whole jet, and on the right- hand side for the parton subjet with momentum k within the angle integral θ). Since the unnormalised moments increase with energy while the parton spectrum decreases, the product $D^\theta \Delta N^{(q)}(k\theta)$ has a maximum at some energy, and the integral over momenta may be calculated by the steepest-descent method. Leaving aside the details of calculations (see Ref. [38]), we describe the general structure of the correlator for the fixed coupling constant $\gamma_0 = \mathrm{const}$:

$$\Delta N^{(q)} \propto \Delta\Omega \left(\frac{\theta_0}{\theta}\right)^{\gamma_0/q} \left(\frac{E\theta}{c}\right)^{q\gamma_0} \qquad (c = \mathrm{const})\,, \tag{105}$$

where the three factors represent the phase space, the energy spectrum factor, and the qth power of the average multiplicity. To get the normalised moment, one must divide expression (105) by the qth power of that part of the mean multiplicity of the whole jet that appears inside the window θ, i.e. by the proportion of the total average multiplicity corresponding to the phase-space volume $\Delta\Omega$:

$$\Delta N(\theta) \propto \Delta\Omega\, \Delta N(\theta_0) \ . \tag{106}$$

If the analysis has been done in the D-dimensional space, the phase-space volume obeys:

$$\Delta\Omega \propto \theta^D \ , \tag{107}$$

where θ corresponds to the minimum linear size on the D-dimensional window that stems from the singular behaviour of parton propagators in QCD (see Ref. [38]). That is why the factorial moments may be represented as products of a purely kinematical factor depending on the dimension of the analysed space, and of the dynamical factor, which is not related to the dimension and defined by the coupling constant

$$F_q \propto \theta^{-D(q-1)} \theta^{(q^2-1/q)\gamma_0} \ . \tag{108}$$

At small angular windows one gets $\theta \sim \delta y$ and the intermittency indices defined by Eqn (103) are given by

$$\phi(q) \ = \ D(q-1) - \frac{q^2-1}{q}\gamma_0 \ . \tag{109}$$

The formula (109) is valid for moderately small windows, in which the condition $\alpha_S \ln\theta_0/\theta < 1$ is fulfilled. For extremely small windows, one should take into account that the coupling constant is running. Then the constant γ_0 should be replaced by the effective value $\langle\gamma\rangle$, which depends logarithmically on the width of the window θ and may be approximated by [38]

$$\langle\gamma\rangle \ = \ \gamma_0\left(1+\frac{\varepsilon}{4}\right) \ , \tag{110}$$

where

$$\varepsilon \ = \ \frac{q^2+1}{q^2}\frac{\ln(\theta_0/\theta)}{\ln(E\theta_0/\mu)} \leqslant 1 \ . \tag{111}$$

As a result, numerical values of the intermittency indices for very small windows become noticeably smaller than in the fixed-coupling regime, especially for the low-rank moments. Moreover, the simple power-law behaviour (103) becomes modified by the logarithmic correction terms and the intermittency indices depend on the value of the chosen interval. The resulting curve of $\ln F_q$ as a function of $-\ln\theta$ has two branches. The rather steep linear increase at the moderately small windows θ with the slope (109) is replaced at smaller window sizes by the much slower quasilinear increase given by Eqns (110) and (111). It is easy to calculate the position of the transition point to another regime and show that, at higher values of q, point shifts to smaller window sizes. Still, the factorial moments of any rank increase at smaller intervals. This demonstrates that the corresponding fluctuations of the multiplicity distributions become stronger than those in larger intervals and, more importantly, noticeably exceed the Poisson fluctuations.

The results of the double-logarithmic approximation have been described. The corrections due to the modified leading-logarithm terms are comparatively small numerically (about 10%). For example, they move the transition point (from power-law to quasipower regime) to slightly smaller windows for any moment except the second one, where it moves to somewhat larger angles. This tendency can be easily prescribed to the mutual influence of the energy spectrum and the average multiplicity. Of more importance are the qualitative effects of new functional dependence on the rank q due to the terms proportional to $q\gamma$. For example, the attempt to exploit the analogy to statistical mechanics [38], where the quantity

$$1 - \frac{\phi(q)+1}{q}$$

is interpreted as 'free energy' and the rank q as an inverse temperature $\beta = 1/kT$, has led to the unexpected result about the 'phase transition'. It shows up because the 'free energy' increases monotonically with q in the lowest-order approximation while higher-order corrections give rise to the maximum just at those q values where H_q has a minimum (71) described above, i.e. at

$$q_{\rm cr} \approx \frac{1}{h_1\gamma_0} \approx 5 \ . \tag{112}$$

In statistical mechanics, this would correspond to zero entropy, i.e. to the phase transition. Here, it just indicates the role of the new parameter $q\gamma$ in QCD as discussed above.

The above results may be restated in terms of fractals. The power-like behaviour of factorial moments suggests fractal properties of particle (parton) distributions in the phase space. According to the general theory of fractals (see Ref. [14] and references therein), the intermittency indices are related to fractal (Renyi) dimensions D_q by the formula

$$\phi(q) \ = \ (q-1)(D-D_q) \ , \tag{113}$$

from which one gets, in the double-logarithmic approximation taking into account Eqn (109),

$$D_q \ = \ \frac{q+1}{q}\gamma_0 \ = \ \gamma_0 + \frac{\gamma_0}{q} \ . \tag{114}$$

The first term corresponds to monofractal behaviour and is due to the average multiplicity increase. The second term provides multifractal properties and is related to the descent of the energy spectrum as discussed above. One can easily obtain the multifractal spectral function in that case (see Ref. [38]). It is clearly seen that the fractality in QCD has a purely dynamical origin ($D_q \sim \gamma_0$) related to the cascade nature of the process, while the kinematical factor in relation (108) has an integer dimension.

The fractality of the particle distributions in the phase-space volume could suggest the fractal properties of colliding objects in ordinary space–time. Surely, owing to its dynamical origin, such a structure would itself be dynamical, i.e. rapidly evolving in space and time. There are two reasons to favour this possibility. First, the cascade process of the evolution of the parton shower in ordinary space must give rise to the 'tree-like' structure of the fractal type which should evolve due to the cascade evolution. Second, the lattice computation in SU(2) gluodynamics [72] has shown that the system of gluons in the vicinity of the phase transition is fractal in the sense that it fills the volume V bounded by the surface S which are related by the formula $V \propto S^{1.12}$. This is typical of fractal objects; the

exponent would be equal to 1.5 for ordinary three-dimensional objects.

The geometric fractality of macroscopic bodies has been revealed by measurements of the power-like shape of the structure functions when some point-like particles (photons, electrons, neutrons, etc) are scattered by them. Using this example, one might try to measure [73] the structure functions in the deep-inelastic processes aiming at the fractal dimensions of the scattered partners. However, this has been done theoretically on the model level only, and experimental difficulties prevent direct comparison. Therefore, the problem of the fractal geometry of particles in ordinary space–time is still waiting to be solved.

Finally, it should be mentioned that no experimental analysis of the noninteger rank moments yet has been performed, and their discussion in Sections 2 and 3 should be interpreted as a rifle in a Chekhov play which is still far from over.

10. Brief discussion of other QCD effects

The theoretical foundation of QCD as a non-Abelian gauge theory describing the interaction of quarks and gluons has been firmly established, though the confinement problem has not yet been resolved. The prediction of asymptotic freedom, i.e. of weaker interaction at small distances, allows one to apply the well-developed methods of perturbation theory. In parallel, there are lattice calculations, some symmetry properties are considered, the potential model approach is developed. The hadronisation of quarks and gluons is described in some models which are compared to experiment if the Monte Carlo calculations are done. The whole arsenal of theoretical methods provides many predictions and describes a lot of effects observed experimentally. Among them there are such successes of QCD as the ratio of the total cross sections of e^+e^- annihilation to hadrons and to the muon pair; predictions of the sum rules, which interrelate quarks of various species; detailed description of the properties of heavy quarkonia; some relations for polarised particles; etc.

The achievements of the perturbative methods have been connected, first, with the hard processes of particle interactions where the transferred momenta are high. Those are the e^+e^- annihilation at high energies, deep-inelastic scattering of leptons and neutrino on hadrons, hadronic processes with large transverse momenta, heavy quark production, and the Drell–Yan process (production of muon pairs with large invariant mass). The universality of the structure functions as applied in various reactions, the correspondence of the lowest approximation of QCD to the parton model results including the scaling property and subsequent violation of it in the higher-order terms due to the running coupling constant were notable landmarks in the evolution of the theory and its comparison to experiment.

The interference effects were studied somewhat later and will be mentioned at some length. The notion of coherence plays a predominant role in many outcomes of theoretical calculations [74, 75]. It is a coherence which allows one to apply the evolution equations for the generating functions considered above on the probabilistic level to the description of jets. One of the most remarkable predictions is the so-called 'hump-backed' plateau [76]. The coherence is especially important for various correlation characteristics (energy flows, multiplicities etc. [10, 35, 71]). Recently, the so-called string [77] or drag [78] effect has been studied experimentally. The theory predicts that in three-jet e^+e^- events there is a depletion of particles in the region between two quarks because they are 'dragged' by the gluon jet while there is no such effect if the photon is emitted in the same direction. This is explained as destructive interference between the two quarks. The analogous effects have been predicted in reactions of creation of photons, muon pairs, and heavy bosons with high transverse momenta.

Another effect of suppression of hadron multiplicity in reactions with heavy quarks has been observed in Ref. [79]. If, compared with the analogous process with the production of light quarks, the so-called companion multiplicity of secondaries in heavy-quark production is several charged particles smaller. By that one means the particles which appear during the hadronisation of bremsstrahlung gluons emitted by the initial quark. The origin of the effect lies in the large masses of heavy quarks. In that case, as is known from scattering theory [80], the radiation of vector particles (in our case, gluons) in the direction of the heavy (or rapidly-decaying) parent is suppressed and the total intensity is reduced. Thus, this observation confirms the vector nature of gluons once again. It would be interesting to measure the angular distribution of such events, which should reveal the ring-like structure of the angular distribution of 'bremsstrahlung' hadrons [81, 82] with a dead cone inside [83].

In general, the idea of the angular ordering of quark–gluon jets due to interference effects is very fruitful and gives rise to the equations for the generating functions of multiplicity distributions considered above.

11. Conclusions

There is a fundamental difference between the effects described in the previous section and the results about multiplicity distributions included in this review. The former are somehow determined by the hardness of the processes, while the multiplicity distributions are mostly related to soft particles appearing at the latest stages of the development of the cascade. Therefore, the success of this approach substantially expands QCD's claims to be able to represent a wide scope. The higher-order approximations for the running coupling constant and the exact solution for the fixed coupling show qualitatively new features of multiplicity distributions, compared with the double-logarithmic approximation. From the physical point of view they should take into account the softer stages of the parton cascade. The qualitative features predicted for partons happen to be valid for hadrons produced both in e^+e^- and hh processes. It prompts speculation about the similarity of the production mechanisms in both cases and about the applicability of higher-order perturbative results to the description of the soft stages.

Evolution of the attitude to extension of the validity region of the perturbative approach can be traced in the history of the problem as described in the introduction. The initial excitement stimulated by predictions of the energy increase of the average multiplicity and of the KNO scaling independent of the coupling constant gave way to some depression evoked by the extremely wide multiplicity distribution predicted theoretically, though it was soon stated that the correction terms were rather large. Now

it becomes completely clear that terms of still higher-order are also important and it is possible to take them into account in a correct way. The results reveal approximate F (or KNO) scaling with dependence on the coupling constant. New features in the behaviour of the moments of multiplicity distributions have been predicted and confirmed by experiment. The evolution of distributions in smaller phase-space regions has also been described. The former discrepancy in the value of the ratio of the average multiplicities in gluon and quark jets has been practically solved. The influence of the higher-order corrections on the energy increase of the average multiplicity has been shown. All these improvements point in the direction of better agreement with experiment.

In combination with predictions of the inclusive spectra and various correlation functions, the above results on the multiplicity distributions tell us that QCD may be successfully applied to predict quite special qualitative features of soft processes when considered in higher orders. Of course, one needs the hadronisation scheme and Monte Carlo calculation to proceed to the quantitative comparison with experiment (which is often substituted by the assumption about the local parton–hadron duality). Unfortunately, they suffer from an abundance of fitting parameters, which are hard to control someTimes. That is why the analytic predictions of new qualitative features and effects are of utmost value. The progress in that direction, described at some length above, gives some hope for further success.

Acknowledgements I am very much indebted to Yu L Dokshitzer, G Gianini, R C Hwa, B B Levtchenko, and V A Nechitailo, with whom I collaborated on the subject.

This work was supported by the Russian Fund for Fundamental Studies (grant 93-02-3815) and by the International Science Foundation (grant M5V000).

References

1. Andreev I V *Khromodinamika i Zhestkie Protsessy pri Vysokikh Energiyakh* (Chromodynamics and Hard Processes at High Energies) (Moscow: Nauka, 1981)
2. Ioffe B L, Lipatov L N, Khoze V A *Glubokoneuprugie Protsessy* (Strongly Inelastic Processes) (Moscow: Energoatomizdat, 1983)
3. Yndurain F J *Quantum Chromodynamics* (Berlin: Springer, 1983)
4. Voloshin M B, Ter-Martirosyan K A *Teoriya Kalibrovochnykh Vzaimodeistvii Elementarnykh Chastits* (Theory of Gauge Interactions of Elementary Particles) (Moscow: Energoatomizdat, 1984)
5. Dokshitzer Yu L, Khoze V A, Mueller A H, Troyan S I *Basics of Perturbative QCD* (Gif-sur-Yvette, France: Editions Frontieres, 1991)
6. Giovannini A, Van Hove L *Z. Phys. C* **30** 391 (1986); *Acta Phys. Pol. B* **19** 495, 917, 931 (1988)
7. Koba Z, Nielsen H B, Olesen P *Nucl. Phys. B* **40** 317 (1972)
8. Azimov Ya I, Dokshitzer Yu L, Khoze V A, Troyan S I *Z. Phys. C* **27** 65 (1985)
9. Amati D, Veneziano G *Phys. Lett. B* **83** 87 (1979)
10. Bassetto A, Ciafaloni M, Marchesini G *Phys. Rep. C* **100** 201 (1983)
11. Bassetto A, Ciafaloni M, Marchesini G *Nucl. Phys. B* **163** 477 (1980)
12. Dokshitzer Yu L *Phys. Lett. B* **305** 295 (1993)
13. Dremin I M *Phys. Lett. B* **313** 209 (1993)
14. De Wolf E A, Dremin I M, Kittel' V *Usp. Fiz. Nauk* **163** 3 (1993); extended version in English *Phys. Rep.* (in press)
15. Friedlander E M, Stern I, Preprint No. LBL-31354 (Berkeley, CA: Lawrence Berkeley Laboratory, 1991)
16. Oldham K *The Fractional Calculus* (Orlando: Academic Press, 1974) p. 60;
    Ross B *Fractional Calculus and its Applications* Lecture Notes in Mathematics, Vol. 457 (Berlin: Springer, 1975) p. 1
17. Dremin I M *Pis'ma Zh. Eksp. Teor. Fiz.* **59** 561 (1994) [*JETP Lett.* **59** 585 (1994)]
18. Cuypers F, Tesima K *Z. Phys. C* **54** 87 (1992)
19. Dokshitzer Yu L, Khoze V A, Troyan S I in *Perturbative QCD* (Ed. A H Mueller) (Singapore: World Scientific, 1989)
20. Dremin I M *Mod. Phys. Lett. A* **8** 2747 (1993)
21. Dremin I M, Hwa R C *Phys. Rev. D* **49** 5805 (1994)
22. Andersson B, Gustafson G, Sjostrand T *Phys. Lett. B* **94** 211 (1980)
23. Andersson B, Gustafson G, Ingelman G, Sjostrand T *Phys. Rep.* **97** 33 (1983)
24. Capella A, Sukhatme U, Tan C I, Tran Thanh Van J *Phys. Lett. B* **81** 68 (1979)
25. Capella A, Tran Thanh Van J *Phys. Lett. B* **93** 146 (1980); *Z. Phys. C* **10** 249 (1981)
26. Kaidalov A B *Phys. Lett. B* **116** 459 (1982)
27. Kaidalov A B, Ter-Martirosyan K A *Phys. Lett. B* **117** 247 (1982); *Yad. Fiz.* **39** 1545; **40** 211 (1984) [*Sov. J. Nucl. Phys.* **39** 979; **40** 135 (1984)]
28. Dremin I M, Dunaevskii A M *Phys. Rep.* **18** 159 (1975)
29. Ugoccioni R, Giovannini A, Lupia S, in *Proceedings of Twenty-Third International Symposium on Multiparticle Dynamics, Aspen, USA, 1993* (Singapore: World Scientific, 1993)
30. Levtchenko B B, Shumilin A V *Z. Phys.* (in Press)
31. Bianchi F, Giovannini A, Lupia S, Ugoccioni R *Z. Phys. C* **58** 71 (1993)
32. Dokshitzer Yu L, Olsson M *Nucl. Phys. B* **396** 137 (1993)
33. Malaza E D, Webber B R *Nucl. Phys. B* **267** 702 (1986)
34. Gaffney J B, Mueller A H *Nucl. Phys. B* **250** 109 (1985)
35. Cuypers F, Tesima K *Z. Phys. C* **52** 69 (1991); **54** 87 (1992)
36. Catani S, Dokshitzer Yu L, Fiorani F, Webber B R *Nucl. Phys. B* **377** 445; **383** 419 (1992)
37. Olsson M, Gustafson G *Nucl. Phys. B* **406** 293 (1993)
38. Dokshitzer Yu L, Dremin I M *Nucl. Phys. B* **402** 139 (1993)
39. Dremin I M, Nechitailo V A *Pis'ma Zh. Eksp. Teor. Fiz.* **58** 945 (1993) [*JETP Lett.* **58** 881 (1993)]
40. Dremin I M, Levtchenko B B, Nechitailo V A *Sov. J. Nucl. Phys.* **57** 1091 (1994)
41. Dremin I M, Nechitailo V A *Mod. Phys. Lett. A* **9** 1471 (1994)
42. Dremin I M, Hwa R C *Phys. Lett. B* **324** 477 (1994)
43. Mueller A H *Nucl. Phys. B* **241** 141 (1984)
44. Malaza E D, Webber B R *Phys. Lett. B* **149** 501 (1984)
45. Marciano W J *Phys. Rev. D* **29** 580 (1984)
46. Dokshitzer Yu L, Khoze V A, Mueller A H, Troyan S I *Rev. Mod. Phys.* **60** 373 (1988)
47. Marchesini G, Webber B R, et al. *Comp. Phys. Comm.* **67** 465 (1992)
48. Gary J W *Phys. Rev. D* **49** 4503 (1994)
49. OPAL collaboration: Acton P D, et al. *Z. Phys. C* **58** 387 (1993)
50. CLEO collaboration: Alam M S, et al. *Phys. Rev. D* **46** 4822 (1992)
51. Gianini G, et al., in *Proccedings of Twenty-Third International Symposium on Multiparticle Dynamics, Aspen, USA, 1993* (Singapore: World Scientific, in press)
52. TASSO collaboration: Braunschweig W, et al. *Z. Phys. C* **45** 193 (1989)
53. HRS collaboration: Derrick M, et al. *Phys. Rev. D* **34** 3304 (1986)
54. ALEPH collaboration: Decamp D, et al. *Phys. Lett. B* **273** 181 (1991)
55. DELPHI collaboration: Abreu P, et al. *Z. Phys. C* **50** 185 (1991)
56. L3 collaboration: Adeva B, et al. *Z. Phys. C* **55** 39 (1992)

57. OPAL collaboration: Acton P D, et al. *Z. Phys. C* **53** 539 (1992)
58. Ammosov V, Boitsov V N, Ermolov P F, et al. *Phys. Lett. B* **42** 519 (1972)
59. Morse W M, Barnes V E, Carmony D D, et al. *Phys. Rev. D* **15** 66 (1977)
60. Charlton G, Cho Y, Derrick M, et al. *Phys. Rev. Lett.* **29** 515 (1972)
61. Firestone A, Davidson V, Lam D, et al. *Phys. Rev. D* **10** 2080 (1974)
62. E743 collaboration: Ammar R, et al. *Phys. Lett. B* **178** 124 (1986)
63. Breakstone A, Campanini R, Crawley H B, et al. *Phys. Rev. D* **30** 528 (1984)
64. UA5 collaboration: Ansorge R E, et al. *Z. Phys. C* **43** 357 (1989)
65. UA5 collaboration: Alner G J, et al. *Phys. Rep.* **154** 247 (1987)
66. Bialas A, Peschanski R *Nucl. Phys. B* **273** 703 (1986)
67. Gustafson G, Nilsson A *Z. Phys. C* **52** 533 (1991); *Nucl. Phys. B* **355** 106 (1991)
68. Ochs W, Wosiek J *Phys. Lett. B* **289** 159 (1992)
69. Ochs W, Wosiek J *Phys. Lett. B* **305** 144 (1993)
70. Brax Ph, Meunier J L, Peschanski R *Z. Phys. C* **62** 649 (1994)
71. Dokshitzer Yu L, Marchesini G, Oriani G *Nucl. Phys. B* **387** 675 (1992)
72. Polikarpov M I *Phys. Lett. B* **236** 61 (1990)
73. Dremin I M, Levtchenko B B *Phys. Lett. B* **292** 155 (1992)
74. Mueller A H *Phys. Lett. B* **104** 161 (1981)
75. Marchesini G, Webber B R *Nucl. Phys. B* **238** 1 (1984)
76. Azimov Ya I, Dokshitzer Yu L, Khoze V A, Troyan S I *Z. Phys. C* **31** 213 (1986)
77. Andersson B, Gustafson G, Sjostrand T *Phys. Lett. B* **94** 211 (1980)
78. Azimov Ya I, Dokshitzer Yu L, Khoze V A, Troyan S I *Phys. Lett. B* **165** 147 (1985)
79. Schumm B A, Dokshitzer Yu L, Khoze V A, Koetke D S *Phys. Rev. Lett.* **69** 3025 (1992)
80. Dremin I M *Pis'ma Zh. Eksp. Teor. Fiz.* **34** 617 (1981) [*JETP Lett.* **34** 594 (1981)]
81. Dremin I M *Pis'ma Zh. Eksp. Teor. Fiz.* **30** 152 (1979) [*JETP Lett.* **20** 140 (1979)]
82. Apanasenko A V, Dobrotin N A, Dremin I M, Kotelnikov K A *Pis'ma Zh. Eksp. Teor. Fiz.*. **30** 157 (1979) [*JETP Lett.* **30** 145 (1979)]
83. Dokshitzer Yu L, Khoze V A, Troyan S I *J. Phys. G* **17** 1481, 1602 (1991)